

**NARA WOMEN'S UNIVERSITY**  
**Graduate School of Humanities and Sciences**  
**Major in Science**



**Spatial Metapopulation Model**  
**As A Point Pattern Dynamics**

**Doctoral Dissertation**

Submitted by

**LE DIEU HUONG**

Student ID: 20970055

Supervisor: **Professor FUGO TAKASU**

**March 2023**

# Contents

<b>Introduction</b>	<b>2</b>
<b>1 Previous studies about metapopulation</b>	<b>4</b>
1.1 Metapopulation . . . . .	4
1.2 Non-spatial metapopulation model . . . . .	8
1.3 Spatial models as lattice models . . . . .	9
1.4 Spatial models as point pattern dynamics . . . . .	10
1.4.1 Definition of point pattern . . . . .	10
1.4.2 Qualification of a point pattern . . . . .	11
<b>2 The Model</b>	<b>15</b>
2.1 Stochastic simulations . . . . .	15
2.2 Dynamics of Singlet and Pair Probabilities . . . . .	19
<b>3 Results</b>	<b>27</b>
3.1 Examples of the point pattern dynamics . . . . .	27
3.2 Dependency of the 1st order equilibrium on parameters . . . . .	37
3.3 Probability of total extinction . . . . .	43
<b>4 Discussion</b>	<b>46</b>
<b>Conclusion</b>	<b>51</b>
<b>Acknowledgement</b>	<b>52</b>
<b>Bibliography</b>	<b>53</b>

# Introduction

In large-scale spatial ecology, there are two lifelong approaches. Firstly, theoretical ecologists have typically investigated a range of models depicting individuals with localized interactions and restricted movement range in homogeneous continuous or discrete (uniform or lattice) space, demonstrating the processes of population dynamics. In the second approach, landscape ecologists tend to be occupied by describing the generally very complex physical structure of real landscapes and less emphasizing on modeling populations dynamics. However, the theoretical ecologists' studies are short of testable model predictions, while landscape ecologists' ones lack a convincing theoretical framework. Therefore, metapopulation ecology was coined for attempting to achieve a compromise between these two approaches above, in which landscapes are viewed as networks of idealized habitat patches (fragmented patches) where species occur as discrete local populations connected by migration (Hanski, 1998 [14]).

The term metapopulation was first given by Richard Levins in 1969 to describe a population of populations, an abstraction of the population concept to a higher level. Studies of metapopulations relate to the equilibrium theory of island biogeography and studies on the dynamics of species living in patchy environments or landscapes. These days, many habitats have become so fragmented that isolated populations cannot be expected to be long-lasting, hence long-term persistence can occur merely via metapopulation dynamics. Therefore, in the conservation of species that are already on the edge of becoming extinct, the metapopulation concept may turn out to be most helpful in the conservation of biodiversity in general in our everyday landscapes. For experimental studies, however, it is costly and time-consuming to collect data from large fragmented environments. Because of that, theoretical studies are useful to give predictions on how metapopulations change with time. Additionally, in reality, local patches are spatially distributed over a space. Therefore, the colonization rate of an empty patch should critically depend on how occupied patches are distributed around it. This solicits the need to explore spatial metapopulation models in which spatial distribution of patches is explicitly considered.

In this research, we analyze a spatial metapopulation model as a stochastic point pattern dynamics. Local patches in our model as points are distributed with a certain spatial configuration and status of each patch changes stochastically between empty and occupied: an empty patch becomes occupied by local and global colonization; an occupied patch becomes empty by local extinction. We implement the stochastic dynamics and carry out simulation analysis. We also derive an analytical model in terms of singlet, pair and triplet probabilities that describe the stochastic dynamics. Using a simple closure that approximates triplet probabilities by singlet and pair probabilities, we show that equilibrium singlet and pair probabilities can be analytically

derived. The derived equilibrium properties successfully describe simulation results under a certain condition where the range of local colonization and the proportion of global colonization play key roles.

Our model is an extension of the classical non-spatial Levins model to a spatially explicit metapopulation model. Point pattern is quite versatile to represent any spatial distribution of local patches. We appeal the advantage of point patterns to study spatial dynamics in general ecology.

**The thesis consists of four chapters:**

Chapter 1: Introducing some background knowledge on metapopulation and relating studies.

Chapter 2: Explaining how we conduct a spatial metapopulation model as a point pattern dynamics. In this chapter we define the model that consists of stochastic simulations and analytical derivations of singlet and pair probabilities describing the stochastic point pattern dynamics of the metapopulation model.

Chapter 3: Showing the results of the model and comparing simulation results with analytical results.

Chapter 4: Discussion about further applications of point pattern approach to study spatial metapopulations and other spatial population dynamics.

# Chapter 1

## Previous studies about metapopulation

In this chapter, we review some introductory knowledge relating to metapopulation models and our research. The content of this chapter consists of a description of metapopulation, metapopulation terminology, non-spatial metapopulation, spatial metapopulation on lattice and an introduction about spatial model as point pattern dynamics.

### 1.1 Metapopulation

The metapopulation concept was introduced by Richard Levins in ecological literature in 1969 [25]. Levins formulated a simple model to investigate the basic dynamics properties of metapopulations (Hanski and Gilpin, 1991 [16]). The term metapopulation is given to describe a population of local populations where interactions occur within each local population and among the local populations. Hence, “the concept of metapopulation is closely connected with the processes of population turnover, extinction and establishment of new populations, and the study of metapopulation dynamics is essentially the study of the conditions under which the extinction and establishment processes are in balance and the consequences of that balance to associated processes” (Hanski, 1991 [13]).

Levins’s metapopulation model has provided a conceptual framework for empirical studies and has served as the starting point of many theoretical analyses (Hanski, 1991 [13]). Studies of metapopulations relate to the equilibrium theory of island biogeography and studies on the dynamics of species living in patchy environments or fragmented landscapes, hence have had important contributions to landscape ecology and conservation biology (Hanski and Gilpin, 1991 [16]; Hanski, 1998 [14]).

There are different types of metapopulation such as classical or Levins metapopulation, patchy metapopulation, mainland-island or non-equilibrium metapopulation (Harrison and Taylor, 1997 [20]) (Figure 1.1).

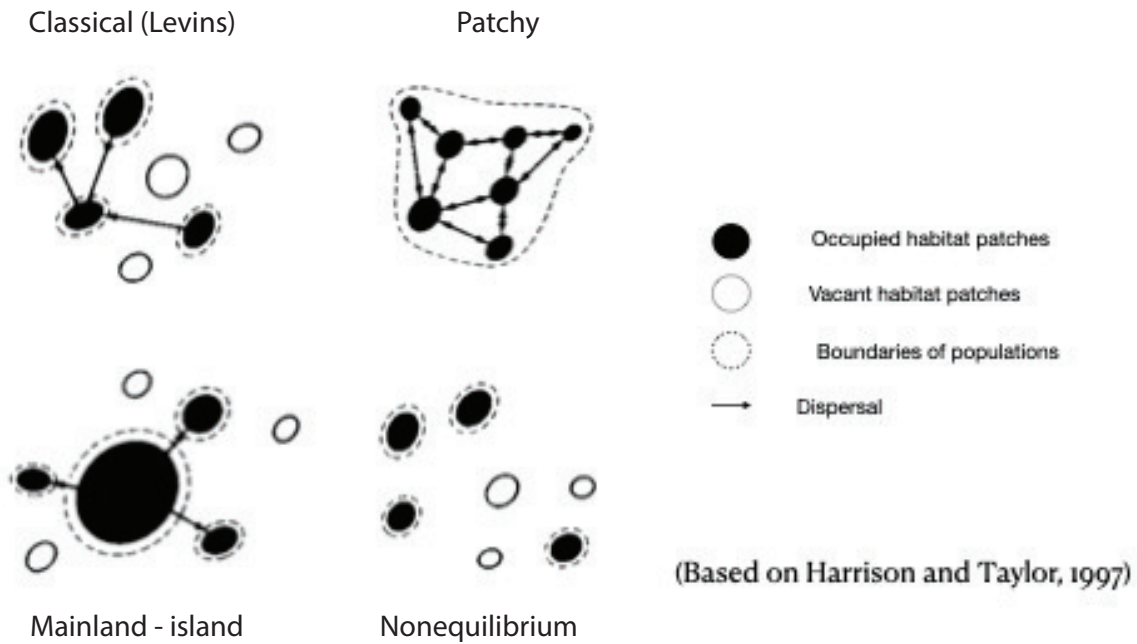


Figure 1.1: Types of metapopulation based on Harrison and Taylor (1997) [20].

Whilst in population studies one focuses on the changes in the number of individuals determined by births and deaths in the population, in the studies of metapopulation we focus on the changes in the status of habitat patches or local populations which are driven by extinction and colonization.

One of typical empirical studies on metapopulations is the large-scale surveys of Glanville fritillary metapopulation that has been conducted since 1993 in the Åland archipelago in Finland (Figure 1.2). Glanville fritillary exemplifies a large number of habitat-specialist species with a metapopulation structure and fast extinction-colonization dynamics in heterogeneous environments (Hanski, 2011 [15]; van Nouhuys, 2016 [35]).



Figure 1.2: Map of the habitat patch network in the Åland Islands (a large network of approximately 4,000 dry meadows) indicate the relative abundance of *Veronica spicata* (larval host species) in the meadows. Circles show the relative abundance of the larva, darker color shows greater relative abundance of *Veronica*, gray shading demonstrates land, and the rest is sea. Data was collected over a period of 18 years from 1993 to 2010 (Hanski, 2011 [15]).

Hanski is well-known for his studies on metapopulation. In Hanski and Gilpin (1991) [16], metapopulation terminology was given as in Table 1.1 in which metapopulations are considered as systems of local populations that are connected by dispersing individuals.

Table 1.1: Metapopulation terminology

Term	Synonyms and definition
Patch	<p><i>Synonyms:</i> Habitat patch, (population) site, locality</p> <p><i>Definition:</i> The area of space within which a local population lives</p>
Local population	<p><i>Definition:</i> Set of individuals which all interact with each other with a high probability</p>
Turnover	<p><i>Synonym:</i> Colonization-extinction dynamics</p> <p><i>Definition:</i> Extinction of local populations and establishment of new populations in empty habitat patches by dispersers from existing local populations</p>
Metapopulation	<p><i>Definition:</i> Set of local populations which interact via individuals moving among populations</p>
Characteristic time scale of metapopulation dynamics	<p><i>Definition:</i> <math>\tau_m = 1/e_{min}</math>, where <math>e_{min}</math> is the lowest extinction rate among local populations</p>
Metapopulation persistence time	<p><i>Synonym:</i> Expected lifetime</p> <p><i>Definition:</i> The length of time until all local populations in a metapopulation have become extinct</p>
Occupancy model	<p><i>Synonyms:</i> Patch model, scalar state model</p> <p><i>Definition:</i> A model in which local population size is ignored and the fraction of habitat patches occupied is modeled. Levin's (1969) model is an occupancy model</p>
Metapopulation structure	<p><i>Synonym:</i> Metapopulation type</p> <p><i>Definition:</i> System of habitat patches which is occupied by a metapopulation and which has a certain distribution of patch sizes and interpatch distances</p>
Structured metapopulation model	<p><i>Synonym:</i> Vector state model</p> <p><i>Definition:</i> A model in which the distribution of local population sizes is modeled</p>

## 1.2 Non-spatial metapopulation model

A simple model for metapopulation dynamics was provided by Levins in which the proportion or fraction of occupied patches changes in continuous time according to an ordinary differential equation model as follows

$$\frac{d}{dt}p = cp(1 - p) - ep, \quad (1.2.1)$$

where  $p$  is the fraction of occupied patches,  $c$  and  $e$  are parameters which set the rates of colonization of current empty patches and local extinction of current occupied patches, respectively. Levins model is equivalent to the logistic growth model; if  $e < c$  then the proportion of occupied patches eventually converges to a positive equilibrium  $p^*$  given as

$$p^* = 1 - \frac{e}{c}. \quad (1.2.2)$$

In Levins model, a single species is considered living in an environment including many similar habitat patches. The local populations occupying these patches is assumed to have the size of either 0 (extinct) or  $K$  (local carrying capacity). All local populations are of the same, constant probability of extinction. Local dynamics and the spatial arrangement of patches are ignored or assumed to have no consequence, that means the movements from an occupied patch are assumed to be equally likely to all other patches.

The Eq. (1.2.1) given by Levins provides a simple model for metapopulation dynamics. It is an analogue to the logistic model as a paradigm of local population growth. The Levins model and the logistic model are indeed structurally similar if we rewrite the Eq. (1.2.1) in the equivalent form

$$\frac{d}{dt}p = (c - e)p \left[ 1 - \frac{p}{1 - \frac{e}{c}} \right]. \quad (1.2.3)$$

The difference  $c - e$  hence gives the rate of increase of  $p$  in a small metapopulation (when  $p$  is small), whereas  $1 - e/c$  is equivalent to local “carrying capacity”, the stable equilibrium point towards which  $p$  moves in time (Hanski and Gilpin, 1991 [16]).

Regarding to the Eq. (1.2.2), although it is simple and obviously limited, it is fundamentally significant to highlight a key aspect of metapopulation dynamics: a metapopulation persists, for a given extinction rate, as long as the colonization rate is greater than a threshold value; and for a given colonization rate, the extinction rate does not exceed a threshold value (Hanski, 1991 [13]).

Levins model is too simple to be directly applied to empirical cases. However, it serves as a conceptual and baseline model from which various models have been analyzed. For instance, Brown and Kodric-Brown (1977) [3] focused on “rescue effect” studying how the probability of local extinction is decreased by immigration. Hanski (1983) [11] studied modifications of Levins model which allows for a varying difference between the local and regional time scales, considering that the rate of local extinction depends on the proportion of occupied patches. Hanski (1985) [12] extended Levins model alternatively by assuming two types of occupied patches,

small and large sized, and showed that a small number of large occupied patches can play a crucial role in the dynamics. Hanski (1991) [13] further considered compensatory effects in which colonization rate and local extinction rate explicitly depend on the degree of isolation and the area of habitat patches.

In [13], Hanski suggested that

It makes two significant simplifying assumptions in Levins model:

- (1) there is no spatial correlation in the status (occupied or not) of habitat patches (the ‘zero-correlation’ assumption), and
- (2) there are only two states, presence and absence (the ‘discrete-state’ assumption with two states).

In reality, spatial correlations in occupancy may arise for two reasons, because dispersal to a nearby patch is more likely than dispersal to a far-away patch (‘stepping-stone’ dispersal), and because extinctions due to some common environmental cause may be spatially correlated.

### 1.3 Spatial models as lattice models

Based on the previous section, although Levins model serves as a conceptual and baseline model, it is non-spatial model and too simple to be directly applied to empirical cases and real systems. As a matter of fact, for more realistic applications, we need to consider some spatial distributions.

As in [32], Sato and Iwasa has emphasized that

Nowadays, the effects of spatial configuration on population and evolutionary processes have been the subject of intensive research efforts in ecology and evolutionary biology. It is now acknowledged that considering spatio-temporal structures spontaneously formed by demographic processes and ecological interactions is sometime essential for understanding population, as well as evolutionary dynamics and that traditional modeling in theoretical ecology assuming complete spatial mixing often fails to capture these dynamics.

Therefore, we have to model spatial metapopulation dynamics. Using “lattice space” is a simple and useful method for modeling metapopulation dynamics in a spatially explicit way. Lattice models are most suitable for metapopulation dynamics of terrestrial plants. Most analyses of these models have used computer simulations of spatial stochastic processes. The results of these computational simulations can be compared with those of mean-field approximations, the traditional models which ignore the spatial structure (Iwasa, 2000 [22]). It is said that mean-field approximation is a common method for simplifying spatial metapopulation dynamics, which completely ignores spatial structure by neglecting the correlation between neighboring sites on the lattice. In this method, local density is assumed to be the same as global density. The mean-field approximation would become exact when the spatial pattern is random.

Typically we assume a lattice space that is regular such as linear, square or triangular, and so on, in which a site is located on a vertex or lattice site and connected with a fixed number of

neighbors sites (Sato et al., 1994 [33]; Iwasa, 2000 [22]; Sato and Iwasa, 2000 [32]). The status of a site changes stochastically depending on that of its own and neighbor sites. A vacant site (denoted by 0) is colonized from adjacent occupied sites (denoted by 1) whereas, an occupied site 1 goes locally extinct to 0. Figure 1.3 illustrates an example of a lattice space with a certain distribution of vacant and occupied sites.

0	0	0	0	0
0	1	1	0	0
0	1	0	0	0
0	0	1	0	0
0	0	0	0	0

Figure 1.3: An example of  $5 \times 5$  square lattice space where 0 and 1 represent empty and occupied cells, respectively. An empty cell can be occupied by colonization from neighboring occupied cell(s)

An analytical approach called “pair approximation” has been developed by Matsuda et al. in 1992 [27] in studies of spatial dynamics of populations on lattice. This is a system of ordinary differential equations yielding average densities and local densities, in which the latter describes the correlation of states of the nearest neighbor cells. However, lattice space is a discrete space and the fact that habitat patches are spatially distributed on regular lattice may be too constrained to apply in real nature.

## 1.4 Spatial models as point pattern dynamics

### 1.4.1 Definition of point pattern

A more natural and flexible approach is to use a mapped point pattern, or simply, a “point pattern” as a collection of points in which a point represents the compositional unit of a population or a metapopulation, e.g., an individual or a local patch. A point pattern is defined as a set of points distributed over continuous space in which each point is assigned a status. For example, in epidemiological SIS models, each point is either susceptible (S) or infectious (I). In metapopulation models, each point is either empty (or vacant) or occupied. While neighbors are straightforward to define for lattice, they are not self-evident for point pattern. Figure 1.4 shows an example of a point pattern where a focal point is observed.

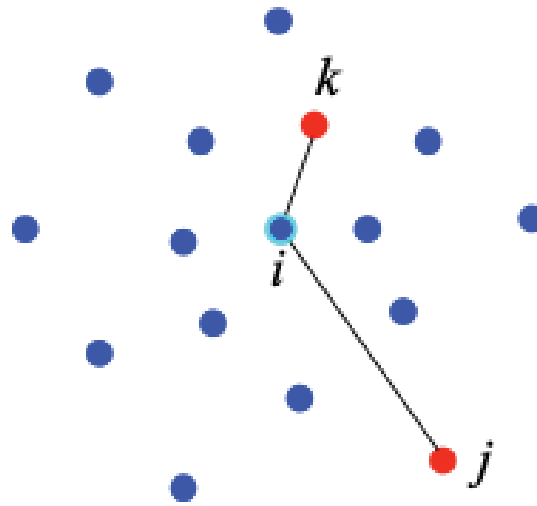


Figure 1.4: An example of a point pattern, in which empty points are in blue, occupied points are in red. The focal blue point  $i$  can be occupied from red points  $j$  and  $k$  with some distance-dependent colonization rate.

Bolker (1999) [1] presented a new analytical model called moment equations for patchy plant epidemics in which the spatial dynamics was considered as stochastic point pattern dynamics. The point pattern approach is shown to be a more natural and general approach to represent a spatial configuration of a metapopulation. A point pattern is considered as consisting of a specific number of points which represent patches on a continuous space. The locations of points defined in two (or three) dimensional space illustrate the spatial configuration of the metapopulation. In order to model metapopulation dynamics we assign each point a status that is either empty (or vacant) or occupied. The same as previous studies relating to lattice models, we focus on a singlet (or a point) and a pair made by two points. However, in the point pattern approach we consider local interactions based on the distance(s) between points with a focal point rather than defining its neighbor points.

## 1.4.2 Qualification of a point pattern

Any point pattern consisting of  $n$  points in two-dimensional space is uniquely represented as a “point” in  $2n$  dimensional space regarding to coordinates of points. For status space, if each point is assigned either empty or occupied in metapopulation model, for example, then we have to work with a  $2^n$  dimensional space. It is intractable to directly deal with such a high dimensional space as the number of points  $n$  increases, especially it is too large in our research as  $n = 1000$ . Fortunately, a new departure in spatial ecology has been introduced to approximate the dynamics of spatial configuration densities in which any point pattern can be characterized using spatial configuration densities that describe the densities of points, pairs, triplets, etc. As the number of points defining such configurations increases (points: 1; pairs: 2; triplets: 3; etc.), successive orders of a spatial point pattern’s information are revealed (Kaito et al., 2015 [23]).

The singlet density describes its first (1st) order structure by the density of points, i.e., by the number of points divided by the area over which they are distributed. Although the singlet density accounts for the abundance of points in a pattern, it is obviously unable to capture any information about how these points are distributed over space. Therefore, the higher-order spatial structure of the pattern has to be considered. Specifically, we need to deal with the second (2nd) order structure of the point pattern that is defined by the densities of pair configurations in order to capture the information about local crowdedness (clustering, aggregation) of points in that pattern. Figure 1.5 demonstrates how we can qualify a point pattern by the number of points, pairs and triplets.

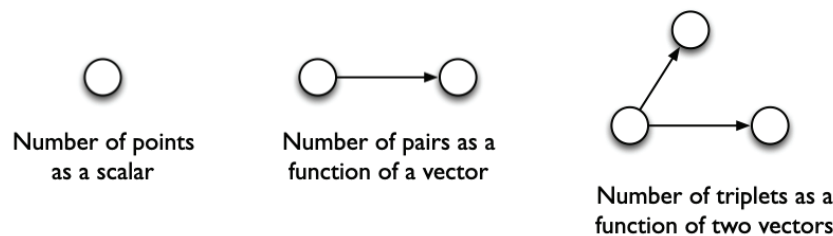


Figure 1.5: Qualification of a point pattern.

A point pattern's pair density is defined as the spatial density of pairs of points dependent on the vector that describes their displacement. In a sufficiently large isotropic point pattern, which exhibits no bias for any particular direction, the density of pairs is uniquely determined by the distance between them. For such patterns, measuring distances among pairs and establishing the distribution of those inter-point distances across all pairs therefore suffices to characterize a pattern's 2nd order structure. More specifically, the degree of clustering of points can be estimated by the following definitions. A pattern is called over-dispersed or regular, if it exhibits a shortage of pairs at short distances, while it is called clustered when it possesses an excess of short-distance pairs. By concentrating on intraspecific (interspecific) pairs formed by two individuals belong to the same (or different) species, salient features of intraspecific (interspecific) interactions at local spatial scale can be inferred.

In [23], Kaito et al. asserted that:

In spatial ecology, measuring the first- and second-order structure (i.e., the singlet and pair densities) of point patterns has been a major interest. Approaches focusing on pairs have been established as powerful tools for quantifying key characteristics of observed point patterns and for unveiling local biological processes underlying such patterns. In tropical forest studies, in particular, these approaches have been successfully applied, providing novel insights about local ecological interactions such as neighborhood competition between trees (Condit, 1998). In response to the resultant increased needs for spatial point-pattern analyses, convenient statistical libraries such as “spatstat” (<http://www.spatstat.org/spatstat/>) are available in R (<http://www.R-project.org/>) to analyze the second-order structure of point patterns.

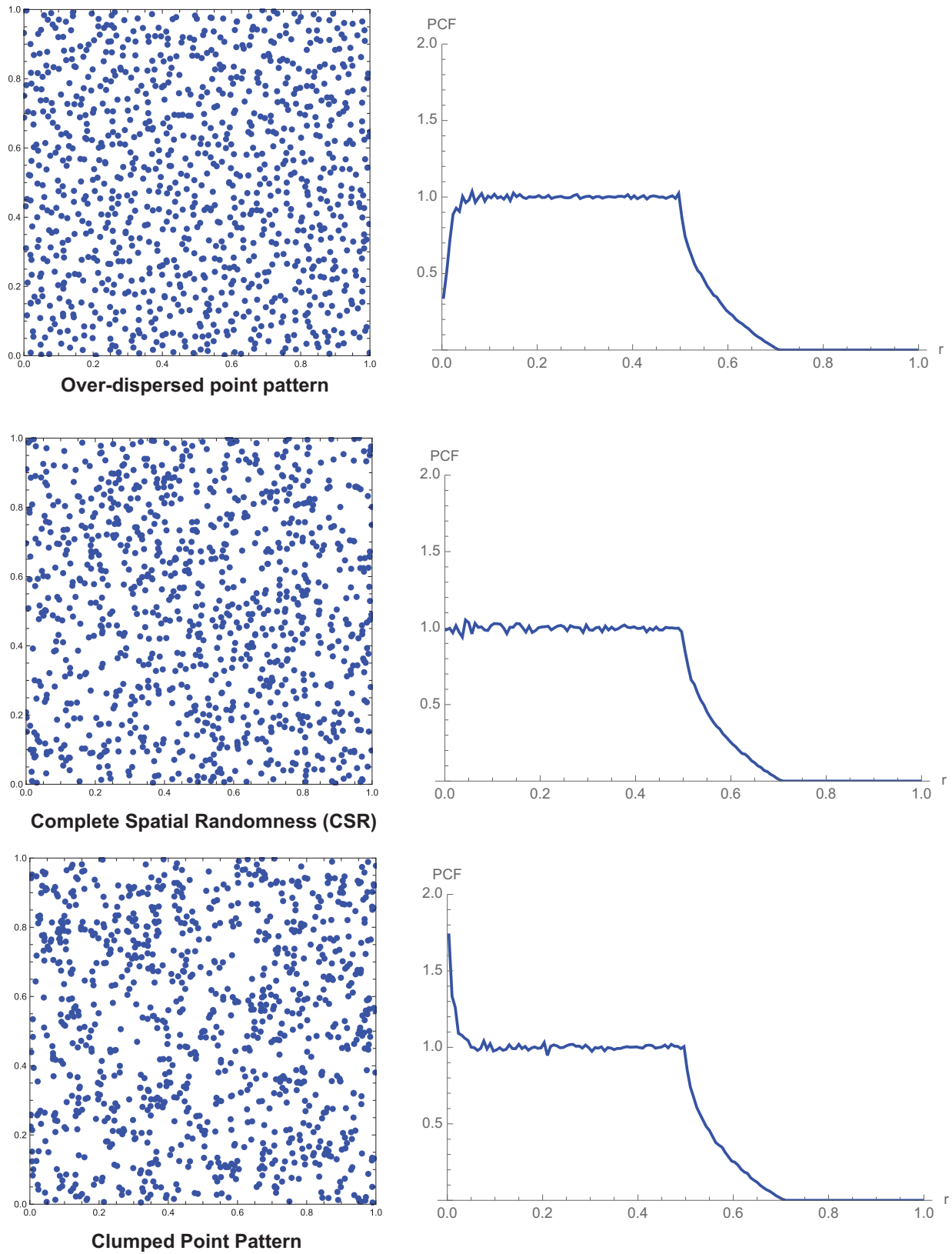


Figure 1.6: Point patterns and corresponding total pair correlation function.

In order to describe the 2nd order structure of the point pattern, we calculate the relative pair correlation function for pairs with a certain pair distance as below. From a snapshot of a point pattern, we count the number of pairs whose pair distance falls within a bin with bin width  $\Delta r$ . Let  $\#(i)$  denote the number of pairs in the  $i$ -th bin. Then we calculate the total pair correlation function as a function of the distance  $r$  representing the  $i$ -th bin  $r_i = \Delta r/2 + i \times \Delta r$  is given as follows

$$g(r_i) = \frac{\#(i)}{2\pi r_i n(n-1)\Delta r}. \quad (1.4.1)$$

On this basis, in Figure 1.6 we show the total pair correlation functions for three types of point pattern called over-dispersed point pattern, complete spatial randomness (or CSR) and clumped point pattern which have been used in many previous studies (we are going to explain in more detail in the next chapter).

# Chapter 2

## The Model

In this chapter, we explain how we conduct a spatial metapopulation model as a point pattern dynamics. Our study stems from Hamada and Takasu (2019) [10] that extended the classical epidemic SIS model as a stochastic point pattern dynamics. Epidemic dynamics and metapopulation dynamics go parallel in the sense that a susceptible  $S$  (empty patch) becomes infectious  $I$  (occupied) by infection (colonization) from another infectious individual(s) and an infectious one recovers to susceptible (local extinction). Hamada and Takasu (2019) [10] studied how infection spread over a point pattern with distance-dependent local infection rate and derived equilibrium properties in terms of singlets and pairs. Applying the same method, we study spatial metapopulation dynamics as a point pattern dynamics with both local and global colonization explicitly considered. We also study the probability of total extinction of the metapopulation starting from one occupied patch.

### 2.1 Stochastic simulations

We first implement our spatial metapopulation dynamics as a stochastic point pattern dynamics. Let us assume a metapopulation that consists of a constant  $n$  patches, each being represented as a point in the two dimensional unit space  $\Omega = [0, 1) \times [0, 1)$  with a certain spatial configuration. We assume that  $\Omega$  is torus with periodic boundary to exclude boundary effects. The location of the  $i$ -th point is represented by the two-dimensional vector  $x_i$  ( $i = 1, 2, \dots, n$ ) in  $\Omega$ . The point pattern  $\{x_1, x_2, \dots, x_n\}$  has been configured according to the pair correlation function or the radial distance distribution  $g(r)$  where  $r$  is the pair-distance. We assume the following three types of point pattern (Figure 2.1):

- An over-dispersed point pattern when  $g(r) < 1$  for short distanced pairs  $r \ll 1$ ,
- Complete spatial randomness (hereafter CSR) with  $g(r) = 1$  for all  $r$ ,
- A clumped point pattern with  $g(r) > 1$  for short distanced pairs  $r \ll 1$ .

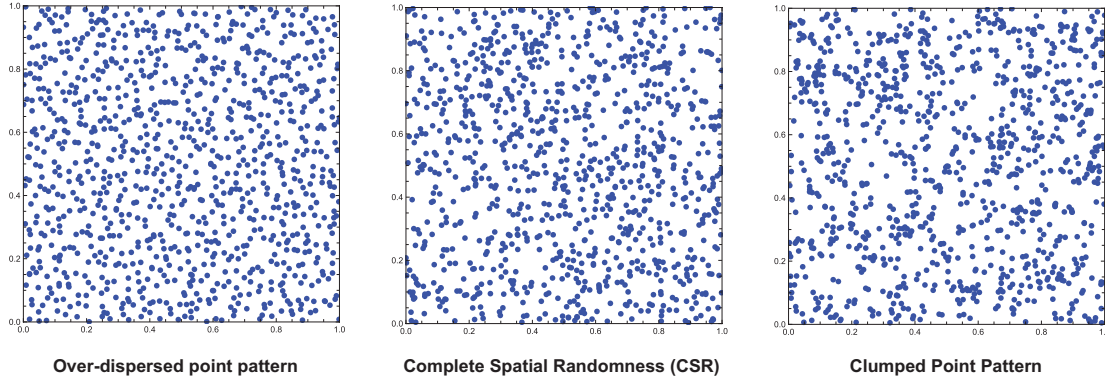


Figure 2.1: Baseline point patterns.

With respect to these three types of point pattern in study, our metapopulation model has a structure, in other words, our spatial model is a kind of structured metapopulation model. Then we assign each point a status either 0 (empty or vacant) or 1 (occupied) and the status changes stochastically in continuous time with colonization and local extinction; a point 0 becomes 1 by colonization and point 1 becomes 0 by local extinction. Thus, our model is also considered as an occupancy model.

We assume that colonization occurs both locally and globally. In local colonization, the distance(s) between a focal empty site and occupied site(s) plays a key role, while in global colonization, distance does not matter. We assume that the colonization rate  $c(d)$  is a function of distance  $d$  between a focal point 0 and a point 1 is given as follows

$$c(d) = (1 - p)c_l(d) + pc_g, \quad (2.1.1)$$

where  $p$  is the proportion of global colonization ( $0 \leq p \leq 1$ ),  $c_l(d)$  and  $c_g$  is the local and the global colonization rate, respectively.

The local colonization rate  $c_l(d)$  is further decomposed as follows

$$c_l(d) = c_{l0}k(d), \quad (2.1.2)$$

where  $c_{l0}$  is the total strength of local colonization and  $k(d)$  is the local colonization kernel that represents how it depends on distance  $d$ .

We assume the following two types of local colonization kernels which are Gaussian and Step-function kernels (Figure 2.2)

$$k(d) = \frac{1}{2\pi\sigma_c^2} \exp\left[-\frac{d^2}{2\sigma_c^2}\right], \quad (2.1.3)$$

$$k(d) = \begin{cases} \frac{1}{4\pi\sigma_c^2} & \text{if } d \leq 2\sigma_c \\ 0 & \text{if } d > 2\sigma_c, \end{cases} \quad (2.1.4)$$

which have been normalized such that integration over the space  $\Omega$  is 1,

$$\int_{\Omega} k(|\xi|)d\xi = 1. \quad (2.1.5)$$

These two kernels have been further normalized so that they have the same effective area of local colonization  $A = 4\pi\sigma_c^2$  (Bolker, 1999 [1]; Brown and Bolker, 2004 [2]; Wright, 1946 [36]) defined as

$$A = \left( \int_{\Omega} [k(|\xi|)]^2 d\xi \right)^{-1}. \quad (2.1.6)$$

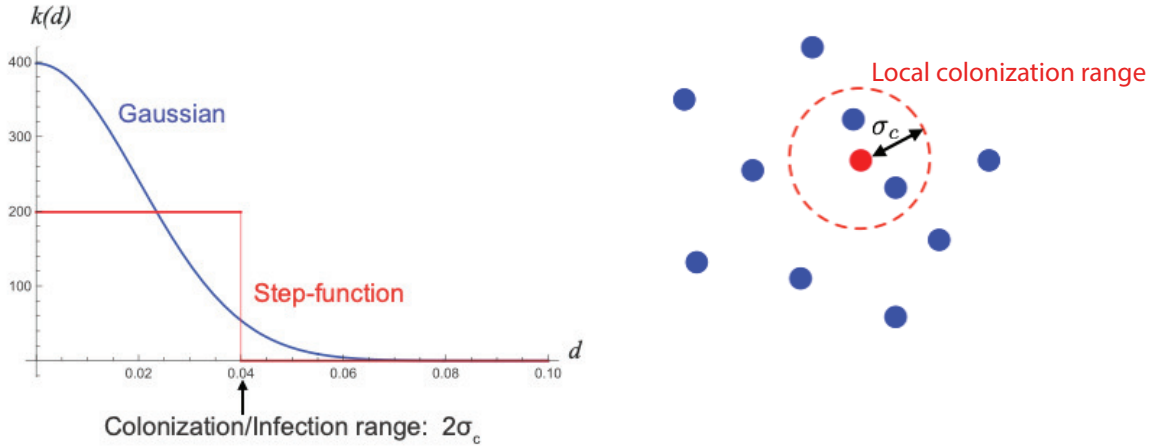


Figure 2.2: The colonization/infection kernel  $k(d)$  as a function of distance  $d$  is shown. Blue and red lines show Gaussian and Step-function respectively.

The Gaussian colonization kernel (2.1.3) assumes that local colonization occurs as a random diffusion process with the parameter  $\sigma_c > 0$  controlling the range of local colonization. The Step function kernel (2.1.4) assumes that local colonization rate remains constant within the radius  $2\sigma_c$  and no local colonization occurs beyond the radius. We choose this kernel as an example of colonization that decays more rapidly with distance than the Gaussian kernel.

Let  $\odot$  denote the set of points whose status is 1 or occupied. Using the colonization rate  $c(d)$  defined above, we define the colonization rate with which the point  $i$  in 0 becomes 1 as

$$\text{Rate}_i(0 \rightarrow 1) = \sum_{j \in \odot} c(d_{ij}), \quad (2.1.7)$$

where  $d_{ij}$  is metric distance between the point  $i$  and  $j$  ( $d_{ij} = |x_i - x_j|$ ) and summation is taken for point  $j$  whose status is 1. Note that the colonization rate above is defined only for points in 0.

We assume that an occupied patch becomes empty by local extinction with a constant rate. We define

$$\text{Rate}_i(1 \rightarrow 0) = e, \quad (2.1.8)$$

where  $e$  is local extinction rate. Note again that the local extinction rate is defined only for points in 1. In addition,  $1/e$  is considered as turnover rate or the mean period occupied status. Also, as the local extinction rate is assumed to be constant and equal to 1, the characteristic time scale of the metapopulation dynamics is unit time 1.

Initially we generate a baseline point pattern with  $n$  points whose pair correlation function is given as  $g(r) = 1 + ae^{-br}$  where the parameters  $a$  and  $b > 0$  control its functional form;  $a = 0$  for CSR,  $a > 0$  for clumped point pattern, and  $a < 0$  for over-dispersed point pattern and  $b$  controls the degree of clumpedness and over-dispersedness (Figure 2.3) (Hamada and Takasu, 2019 [10]). To generate such a point pattern we use Metropolis-Hasting algorithm (Kaito et al., 2015 [23]). We then introduce one occupied 1 patch randomly chosen among empty 0 patches. We update each point status using Gillespie algorithm (Gillespie, 1976 [9]).

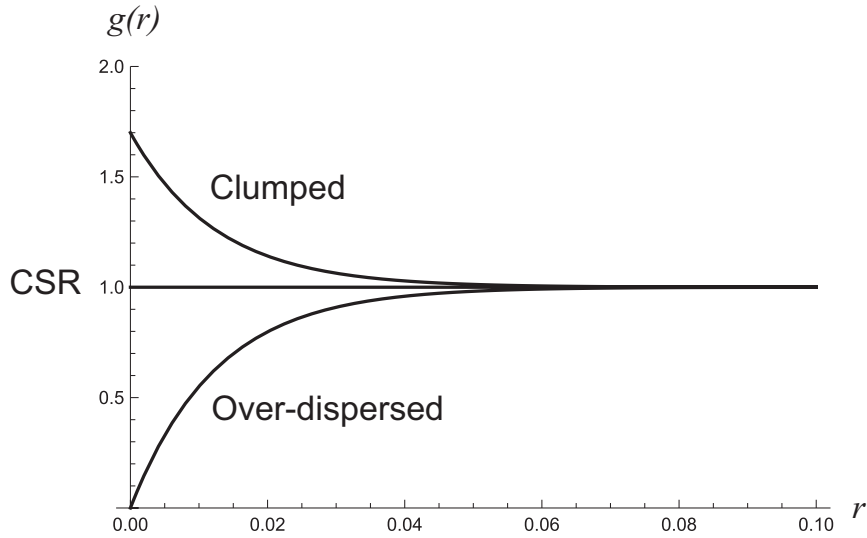


Figure 2.3: Pair correlation function,  $g(r) = 1 + a \exp(-br)$ ; CSR ( $g(r) = 1$ ); over-dispersed ( $g(r) = 1 - \exp(-80r) < 1$ ); and clumped ( $g(r) = 1 + 0.7 \exp(-80r) > 1$ ).

In order to quantify the point pattern, we study the 1st order and 2nd order structure of the point pattern. Regarding to the 1st order, we calculate the number or the proportion of occupied points (1s) and empty points (0s). As the 1st order structure is not adequate for describing how 1s and 0s are spatially distributed over space, we need to consider the 2nd order structure which study the pair correlation function or the radial distance distribution as the distribution of distances in pair made by two points (Dale and John, 1999[6]; Diggle, 2003 [8]; Levin, 1992 [24]; Liebhold and Gurevitch, 2002 [26]; Turner, 1989 [34]). To describe the 2nd order structure of the point pattern, we follow the same definition of relative pair correlation functions for four status of pairs (Hamada and Takasu, 2019 [10]) with a certain pair distance as below.

For a snapshot of a point pattern, we count the number of pairs whose pair distance falls within a bin with bin width  $\Delta r$ . We denote  $\#_{11}(i)$ ,  $\#_{10}(i)$ ,  $\#_{01}(i)$ , and  $\#_{00}(i)$  as the number of directed pairs 1-1, 1-0, 0-1, and 0-0 in the  $i$ -th bin, respectively. Note that  $\#_{10}(i) = \#_{01}(i)$ . Then we calculate relative pair correlation functions for the four types of pairs. E.g., for 1-1 pairs,  $g_{11}(r)$  as a function of the distance  $r$  representing the  $i$ -th bin  $r_i = \Delta r/2 + i \times \Delta r$  is given as follows

$$g_{11}(r_i) = \frac{\#_{11}(i)}{2\pi r_i n(n-1)\Delta r}. \quad (2.1.9)$$

Relative pair correlation functions for pairs 1-0, 0-1, and 0-0,  $g_{10}(r_i)$ ,  $g_{01}(r_i)$ , and  $g_{00}(r_i)$ , are derived similarly. Since the pair correlation function  $g(r)$  represents the spatial distribution of the point pattern in use (for example,  $g(r) = 1$  corresponds to CSR), the relative pair correlation functions defined as above illustrates how points 1s and 0s are distributed over space. Note that  $g(r) = g_{11}(r) + g_{10}(r) + g_{01}(r) + g_{00}(r)$ .

Without loss of generality, we set  $c_{10} = c_g$ . In the absence of global colonization rate  $p = 0$ , our model is reduced to the model of Hamada and Takasu (2019) [10].

## 2.2 Dynamics of Singlet and Pair Probabilities

In this section, we derive the dynamics that describes the stochastic point pattern dynamics in terms of singlets and pairs. Let  $P_{i0}(t)$  and  $P_{i1}(t)$  denote the probability that the point  $i$  is in 0 and 1 at time  $t$ , respectively, and we call them singlet probabilities ( $P_{i0}(t) + P_{i1}(t) = 1$  for  $i = 1, 2, \dots, n$ ). In addition, we define the average (mean-field) singlet probabilities

$$\langle P_0 \rangle = \frac{1}{n} \sum_{i=1}^n P_{i0}, \quad \langle P_1 \rangle = \frac{1}{n} \sum_{i=1}^n P_{i1} \quad (2.2.1)$$

as the proportion of empty and occupied patches.

When we choose two points  $i$  and  $j$  ( $j \neq i$ ), we have a directed pair  $i$ - $j$  represented by the vector  $\xi_{ij} = x_j - x_i$  with the distance  $d_{ij} = |\xi_{ij}|$ . We denote the probability that the directed pair  $i$ - $j$  is in status 0-0, 0-1, 1-0, and 1-1 at time  $t$  by  $P_{ij00}(t)$ ,  $P_{ij01}(t)$ ,  $P_{ij10}(t)$  and  $P_{ij11}(t)$ , respectively and call them pair probabilities ( $P_{ij00}(t) + P_{ij01}(t) + P_{ij10}(t) + P_{ij11}(t) = 1$  for  $i \neq j$ ).

Since each point can be in one of two status 0 and 1, there are four types of status for a directed pair  $i$  and  $j$  ( $j \neq i$ ) which are 1-1, 1-0, 0-1 and 0-0. Using the transition diagram of singlets and pairs in Figure 2.4 we derive the singlet dynamics. Because  $P_{i0} + P_{i1} = 1$ , we hereafter focus on the dynamics of  $P_{i1}$ . The singlet dynamics of the point  $i$  is given as follows (Hamada and Takasu, 2019 [10])

$$\frac{d}{dt} P_{i1} = -e P_{i1} + (1-p) \sum_{j \neq i} c_l(d_{ij}) P_{ij01} + p c_g \sum_{j \neq i} P_{ij01} \quad (2.2.2)$$

for  $i = 1, 2, \dots, n$ .

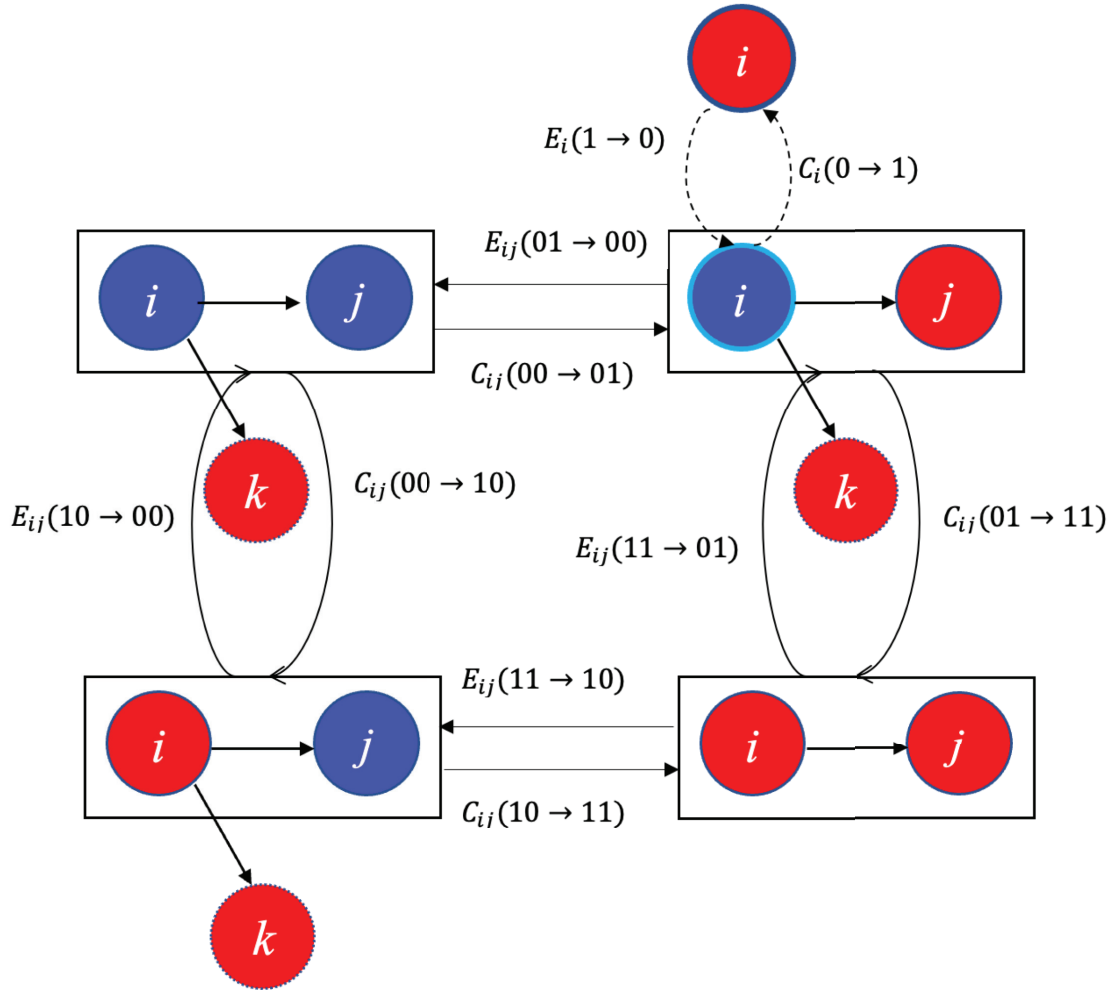


Figure 2.4: Transition Diagram. Empty (0) points are in blue, occupied (1) points are in red.

On the right hand side of Eq. (2.2.2), the first term represents the local extinction that is assumed to occur with the constant rate  $e$ . The second term represents the local colonization depending on distance(s) from occupied patches; the point  $i$  in 0 is colonized locally from the point  $j$  in 1 with the local colonization rate  $(1-p)c_l(d_{ij})$  summed over all possible  $j \neq i$ . The last term represents the global colonization that has been assumed distance-independent. In Eq. (2.2.2), however, this distance-independency of global colonization is not satisfied because  $P_{ij01} = P_{i0}P_{j1|i0} \neq P_{i0}P_{j1}$  in general where  $P_{j1|i0}$  is conditional probability: the point  $j$  is 1 conditional on that the point  $i$  is 0. This inconsistency can be safely handled by decoupling the point  $i$  and  $j$  by setting  $P_{j1|i0} = P_{j1}$  because the last term as global colonization assumes no correlation between the two points  $i$  and  $j$ . Then, we apply the following approximation

$$\sum_{j \neq i} P_{ij01} = \sum_{j \neq i} P_{i0}P_{j1|i0} = P_{i0} \sum_{j \neq i} P_{j1} \approx P_{i0}(n-1)\langle P_1 \rangle \approx nP_{i0}\langle P_1 \rangle$$

for  $n$  being large enough.

Finally we obtain the singlet dynamics

$$\frac{d}{dt}P_{i1} = -eP_{i1} + (1-p) \sum_{j \neq i} c_l(d_{ij})P_{ij01} + pc_g n \langle P_1 \rangle P_{i0} \quad (2.2.3)$$

for  $i = 1, 2, \dots, n$  and the mean-field singlet dynamics

$$\frac{d}{dt} \langle P_1 \rangle = -e \langle P_1 \rangle + (1-p) \frac{1}{n} \sum_{i=1}^n \sum_{j \neq i} c_l(d_{ij})P_{ij01} + pc_g n \langle P_0 \rangle \langle P_1 \rangle. \quad (2.2.4)$$

Note that the classical Levins model (Levins, 1969 [25]) can be obtained when we set  $p = 1$  in the Eq. (2.2.4).

The singlet dynamics contains the pair probability  $P_{ij01}$ . We next derive the dynamics of the pair probabilities. Using the approach of Hamada and Takasu (2019) [10] and the transition diagram as in Figure 2.4, the dynamics of the pair probabilities  $P_{ij00}, P_{ij01}, P_{ij10}$ , and  $P_{ij11}$  are given as follows

$$\begin{aligned} \frac{d}{dt}P_{ij00} = & -(1-p) \sum_{k \neq i,j} c_l(d_{ik})P_{ijk001} - (1-p) \sum_{k \neq i,j} c_l(d_{jk})P_{ijk001} - 2pc_g n \langle P_1 \rangle P_{ij00} \\ & + eP_{ij01} + eP_{ij10}, \end{aligned} \quad (2.2.5)$$

$$\begin{aligned} \frac{d}{dt}P_{ij01} = & -(1-p) \sum_{k \neq i,j} c_l(d_{ik})P_{ijk011} + (1-p) \sum_{k \neq i,j} c_l(d_{jk})P_{ijk001} + pc_g n \langle P_1 \rangle P_{ij00} \\ & - pc_g n \langle P_1 \rangle P_{ij01} - (1-p)c_l(d_{ij})P_{ij01} - pc_g P_{ij01} - eP_{ij01} + eP_{ij11}, \end{aligned} \quad (2.2.6)$$

$$\begin{aligned} \frac{d}{dt}P_{ij10} = & (1-p) \sum_{k \neq i,j} c_l(d_{ik})P_{ijk001} - (1-p) \sum_{k \neq i,j} c_l(d_{jk})P_{ijk101} + pc_g n \langle P_1 \rangle P_{ij00} \\ & - pc_g n \langle P_1 \rangle P_{ij10} - (1-p)c_l(d_{ij})P_{ij10} - pc_g P_{ij10} - eP_{ij10} + eP_{ij11}, \end{aligned} \quad (2.2.7)$$

$$\begin{aligned} \frac{d}{dt}P_{ij11} = & (1-p) \sum_{k \neq i,j} c_l(d_{ik})P_{ijk011} + (1-p) \sum_{k \neq i,j} c_l(d_{jk})P_{ijk101} \\ & + (1-p)c_l(d_{ij})P_{ij01} + pc_g P_{ij01} + (1-p)c_l(d_{ij})P_{ij10} + pc_g P_{ij10} \\ & + pc_g n \langle P_1 \rangle P_{ij01} + pc_g n \langle P_1 \rangle P_{ij10} - 2eP_{ij11}. \end{aligned} \quad (2.2.8)$$

Taking the dynamics of  $P_{ij11}$  as an example, Eq.(2.2.8) describes how a pair 1-1 is generated or lost; a pair 1-1 is newly generated from a pair 1-0 or 0-1 by colonization; the point 0 in the pair is colonized by a third party point  $k \neq i, j$  in 1 or by within-pair colonization, and is lost by local extinction in the pair. Therefore, the pair dynamics involves triplet probabilities;  $P_{ijk001}$ ,  $P_{ijk011}$ , and  $P_{ijk101}$  are the probabilities that the triplet  $i-j-k$  ( $i \neq j \neq k$ ) is in status 0-0-1, 0-1-1, and 1-0-1, respectively.

It should be noted that the singlet and the pair dynamics derived above apparently do not depend on spatial configuration of the point pattern used (CSR, clumped, or over-dispersed) and thus the pair correlation function  $g(r)$  of the baseline point pattern is not explicitly involved. However, the dynamics does depend on  $g(r)$  through summation of local colonization for pairs and triplets as shown later.

The singlet and the pair dynamics are not self-contained; triplet probabilities appear in the dynamics. To close the dynamics, we need to assume triplet probabilities to be approximated by lower order singlet and pair probabilities. We adopt the following simple closures (Dieckmann and Law, 2000 [7], Hamada and Takasu, 2019 [10]) because these allow us to derive equilibrium pair probabilities analytically.

$$\begin{aligned}
P_{ijk001} &= \frac{P_{ij00}P_{ik01}}{\langle P_0 \rangle} \text{ for the point } i \text{ as pivot,} \\
P_{ijk001} &= \frac{P_{ji00}P_{jk01}}{\langle P_0 \rangle} = \frac{P_{ij00}P_{jk01}}{\langle P_0 \rangle} \text{ for the point } j \text{ as pivot,} \\
P_{ijk011} &= \frac{P_{ij01}P_{ik01}}{\langle P_0 \rangle} \text{ for the point } i \text{ as pivot,} \\
P_{ijk101} &= \frac{P_{ji01}P_{jk01}}{\langle P_0 \rangle} = \frac{P_{ij10}P_{jk01}}{\langle P_0 \rangle} \text{ for the point } j \text{ as pivot.}
\end{aligned} \tag{2.2.9}$$

In the above closures, we focus on a focal point whose status changes from 0 to 1 in a triplet. The triplet is then viewed from the focal point as ‘‘pivot’’ and we approximate the triplet probability using two pair probabilities stemming from the focal point and the mean-field singlet probability of the focal point (Figure 2.5).

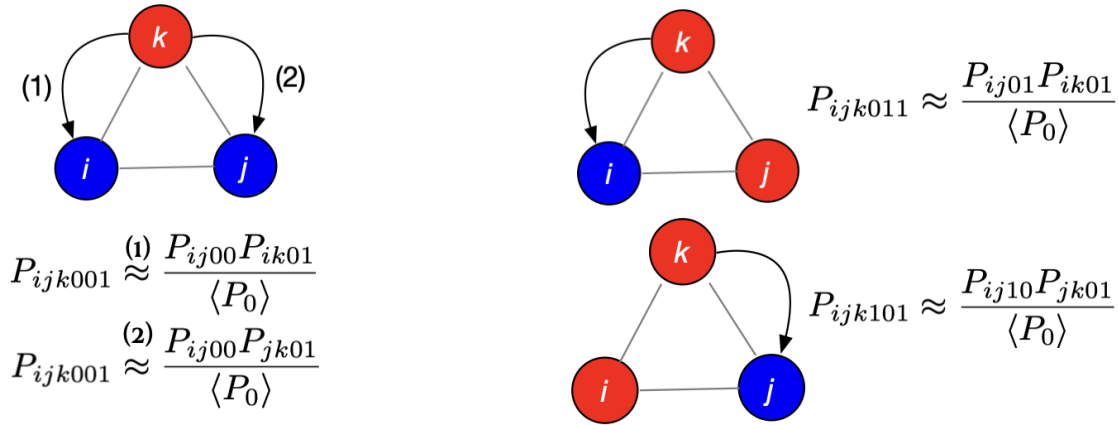


Figure 2.5: Triplet probabilities are approximated by coupled pair probabilities using moment closure with the consideration of focal point.

For example, in the summation  $\sum_{k \neq i, j} c_l(d_{ik})P_{ijk001}$  in the pair dynamics, the point  $i$  is considered as pivot and we have

$$\begin{aligned}
\sum_{k \neq i, j} c_l(d_{ik})P_{ijk001} &= \sum_{k \neq i, j} c_l(d_{ik}) \frac{P_{ij00}P_{ik01}}{\langle P_0 \rangle} \\
&= \frac{P_{ij00}}{\langle P_0 \rangle} \sum_{k \neq i, j} c_l(d_{ik})P_{ik01}.
\end{aligned}$$

Whereas, in the summation  $\sum_{k \neq i, j} c_l(d_{jk})P_{ijk001}$ ,  $j$  is pivot and we have

$$\begin{aligned} \sum_{k \neq i, j} c_l(d_{jk})P_{ijk001} &= \sum_{k \neq i, j} c_l(d_{jk})P_{jki010} \\ &= \sum_{k \neq i, j} c_l(d_{jk}) \frac{P_{ji00}P_{jk01}}{\langle P_0 \rangle} \\ &= \frac{P_{ji00}}{\langle P_0 \rangle} \sum_{k \neq i, j} c_l(d_{jk})P_{jk01}. \end{aligned}$$

Similarly, we have

$$\begin{aligned} \sum_{k \neq i, j} c_l(d_{ik})P_{ijk011} &= \frac{P_{ij01}}{\langle P_0 \rangle} \sum_{k \neq i, j} c_l(d_{ik})P_{ik01}, \\ \sum_{k \neq i, j} c_l(d_{jk})P_{ijk101} &= \frac{P_{ij10}}{\langle P_0 \rangle} \sum_{k \neq i, j} c_l(d_{jk})P_{jk01}. \end{aligned}$$

Substituting the closures Eqs. (2.2.9) to the dynamics of pair probabilities Eq.(2.2.5) through Eq.(2.2.8), and setting the time derivative zero, we obtain the following equations from which equilibrium pair probabilities can be solved

$$0 = \frac{d}{dt}P_{ij00} = \left[ -\frac{1-p}{\langle P_0 \rangle} \left( \sum_{k \neq i, j} c_l(d_{ik})P_{ik01} + \sum_{k \neq i, j} c_l(d_{jk})P_{jk01} \right) - 2pc_g n \langle P_1 \rangle \right] P_{ij00} + eP_{ij01} + eP_{ij10}, \quad (2.2.10)$$

$$\begin{aligned} 0 = \frac{d}{dt}P_{ij01} &= \left[ \frac{1-p}{\langle P_0 \rangle} \sum_{k \neq i, j} c_l(d_{jk})P_{jk01} + pc_g n \langle P_1 \rangle \right] P_{ij00} + eP_{ij11} \\ &+ \left[ -\frac{(1-p)}{\langle P_0 \rangle} \sum_{k \neq i, j} c_l(d_{ik})P_{ik01} - e - (1-p)c_l(d_{ij}) - pc_g - pc_g n \langle P_1 \rangle \right] P_{ij01}, \end{aligned} \quad (2.2.11)$$

$$\begin{aligned} 0 = \frac{d}{dt}P_{ij10} &= \left[ \frac{1-p}{\langle P_0 \rangle} \sum_{k \neq i, j} c_l(d_{ik})P_{ik01} + pc_g n \langle P_1 \rangle \right] P_{ij00} + eP_{ij11} \\ &+ \left[ -\frac{1-p}{\langle P_0 \rangle} \sum_{k \neq i, j} c_l(d_{jk})P_{jk01} - e - (1-p)c_l(d_{ij}) - pc_g - pc_g n \langle P_1 \rangle \right] P_{ij10}, \end{aligned} \quad (2.2.12)$$

$$\begin{aligned} 0 = \frac{d}{dt}P_{ij11} &= \left[ \frac{1-p}{\langle P_0 \rangle} \sum_{k \neq i, j} c_l(d_{ik})P_{ik01} + (1-p)c_l(d_{ij}) + pc_g + pc_g n \langle P_1 \rangle \right] P_{ij01} \\ &+ \left[ \frac{1-p}{\langle P_0 \rangle} \sum_{k \neq i, j} c_l(d_{jk})P_{jk01} + (1-p)c_l(d_{ij}) + pc_g + pc_g n \langle P_1 \rangle \right] P_{ij10} - 2eP_{ij11}. \end{aligned} \quad (2.2.13)$$

Here, we approximate the terms  $\sum_{k \neq i, j} c_l(d_{ik})P_{ik01}$  and  $\sum_{k \neq i, j} c_l(d_{jk})P_{jk01}$  with the mean-field value

$$\begin{aligned} \sum_{k \neq i, j} c_l(d_{ik})P_{ik01} &\approx \frac{1}{n} \sum_{i=1}^n \sum_{k \neq i} c_l(d_{ik})P_{ik01}, \\ \sum_{k \neq i, j} c_l(d_{jk})P_{jk01} &\approx \frac{1}{n} \sum_{j=1}^n \sum_{k \neq j} c_l(d_{jk})P_{jk01}. \end{aligned} \quad (2.2.14)$$

And using the equilibrium condition of the singlet dynamics

$$0 = \frac{d}{dt} \langle P_1 \rangle = -e \langle P_1 \rangle + (1-p) \frac{1}{n} \sum_{i=1}^n \sum_{j \neq i} c_l(d_{ij})P_{ij01} + pc_g n \langle P_0 \rangle \langle P_1 \rangle, \quad (2.2.15)$$

we have

$$\frac{1}{n} \sum_{i=1}^n \sum_{j \neq i} c_l(d_{ij})P_{ij01} = \frac{1}{1-p} [e \langle P_1 \rangle - pc_g n \langle P_0 \rangle \langle P_1 \rangle]. \quad (2.2.16)$$

From Eq.(2.2.14) and Eq.(2.2.16) we get

$$\begin{aligned} \sum_{k \neq i, j} c_l(d_{ik})P_{ik01} &\approx \frac{1}{1-p} [e \langle P_1 \rangle - pc_g n \langle P_0 \rangle \langle P_1 \rangle], \\ \sum_{k \neq i, j} c_l(d_{jk})P_{jk01} &\approx \frac{1}{1-p} [e \langle P_1 \rangle - pc_g n \langle P_0 \rangle \langle P_1 \rangle]. \end{aligned}$$

Hence the equations for deriving the equilibrium of pair probabilities can be simplified in matrix and vector notation as follows

$$\mathbf{A} \begin{pmatrix} P_{ij00} \\ P_{ij01} \\ P_{ij10} \\ P_{ij11} \end{pmatrix} = \begin{pmatrix} 0 \\ 0 \\ 0 \\ 0 \end{pmatrix}, \quad (2.2.17)$$

in which  $\mathbf{A}$  is a  $4 \times 4$  matrix

$$\begin{pmatrix} -2e \frac{\langle P_1 \rangle}{\langle P_0 \rangle} & e & e & 0 \\ e \frac{\langle P_1 \rangle}{\langle P_0 \rangle} & -e - (1-p)c_l(d_{ij}) - pc_g - e \frac{\langle P_1 \rangle}{\langle P_0 \rangle} & 0 & e \\ e \frac{\langle P_1 \rangle}{\langle P_0 \rangle} & 0 & -e - (1-p)c_l(d_{ij}) - pc_g - e \frac{\langle P_1 \rangle}{\langle P_0 \rangle} & e \\ 0 & (1-p)c_l(d_{ij}) + pc_g + e \frac{\langle P_1 \rangle}{\langle P_0 \rangle} & (1-p)c_l(d_{ij}) + pc_g + e \frac{\langle P_1 \rangle}{\langle P_0 \rangle} & -2e \end{pmatrix}. \quad (2.2.18)$$

The matrix  $\mathbf{A}$  is singular and Eq.(2.2.17) has no unique solution. But all pair probabilities have to sum up to one and we obtain the equilibrium pair probabilities for all pairs  $i$ - $j$  ( $i \neq j$ ) as shown in Eq.(2.2.19) through Eq.(2.2.22) as follows

$$P_{ij00} = \frac{e\langle P_0 \rangle^2}{e + [(1-p)c_l(d_{ij}) + pc_g]\langle P_0 \rangle \langle P_1 \rangle} = P_{00}(d_{ij}), \quad (2.2.19)$$

$$P_{ij01} = \frac{e\langle P_0 \rangle \langle P_1 \rangle}{e + [(1-p)c_l(d_{ij}) + pc_g]\langle P_0 \rangle \langle P_1 \rangle} = P_{01}(d_{ij}), \quad (2.2.20)$$

$$P_{ij10} = \frac{e\langle P_1 \rangle \langle P_0 \rangle}{e + [(1-p)c_l(d_{ij}) + pc_g]\langle P_0 \rangle \langle P_1 \rangle} = P_{10}(d_{ij}), \quad (2.2.21)$$

$$P_{ij11} = \frac{e\langle P_1 \rangle^2 + [(1-p)c_l(d_{ij}) + pc_g]\langle P_0 \rangle \langle P_1 \rangle}{e + [(1-p)c_l(d_{ij}) + pc_g]\langle P_0 \rangle \langle P_1 \rangle} = P_{11}(d_{ij}). \quad (2.2.22)$$

where  $d_{ij}$  is the distance between the point  $i$  and  $j$ .

However, the mean-field singlet probabilities  $\langle P_0 \rangle$  and  $\langle P_1 \rangle$  have not been determined yet. Substituting Eq. (2.2.20) to Eq. (2.2.16), we get

$$-e\langle P_1 \rangle + pc_g n \langle P_0 \rangle \langle P_1 \rangle + \frac{1-p}{n} \sum_{i=1}^n \sum_{j \neq i} c_l(d_{ij}) \frac{e\langle P_0 \rangle \langle P_1 \rangle}{e + [(1-p)c_l(d_{ij}) + pc_g]\langle P_0 \rangle \langle P_1 \rangle} = 0. \quad (2.2.23)$$

The double summation for  $j \neq i$  and for  $i$  in Eq. (2.2.23) can be replaced with the summation for all directed pairs ( $i \neq j$ ) as  $d_{ij} = |\xi_{ij}| = |\xi_m|$  indexed by  $m = 1, 2, \dots, n(n-1)$ . Rearranging this equation, we obtain an equation to solve the equilibrium mean field singlet probability  $\langle P_1 \rangle$  as follows

$$1 = \frac{p}{e} c_g n \langle P_0 \rangle + \frac{1-p}{n} \sum_{m=1}^{n(n-1)} \frac{c_l(d_m) \langle P_0 \rangle}{e + [(1-p)c_l(d_m) + pc_g]\langle P_0 \rangle \langle P_1 \rangle}. \quad (2.2.24)$$

The distribution of the distances in pairs  $r = |\xi_m| = d_m$  is proportional to  $2\pi r g(r)$  and the total number of directed pairs is  $n(n-1)$ . Hence, Eq. (2.2.24) can be approximated as

$$1 \approx \frac{p}{e} c_g n (1 - \langle P_1 \rangle) + (1-p)(n-1) \int_0^\infty \frac{c_l(r)(1 - \langle P_1 \rangle)}{e + [(1-p)c_l(r) + pc_g](1 - \langle P_1 \rangle)\langle P_1 \rangle} 2\pi r g(r) dr. \quad (2.2.25)$$

The right hand side of Eq. (2.2.25) is a function of averaged singlet probability  $\langle P_1 \rangle$ , saying function  $F$ . It is a monotonically decreasing function of  $\langle P_1 \rangle$

$$F(\langle P_1 \rangle) = \frac{p}{e} c_g n (1 - \langle P_1 \rangle) + (1 - p)(n - 1) \int_0^\infty \frac{c_l(r)(1 - \langle P_1 \rangle)}{e + [(1 - p)c_l(r) + pc_g](1 - \langle P_1 \rangle)\langle P_1 \rangle} 2\pi r g(r) dr \quad (2.2.26)$$

with  $F(1) = 0$ .

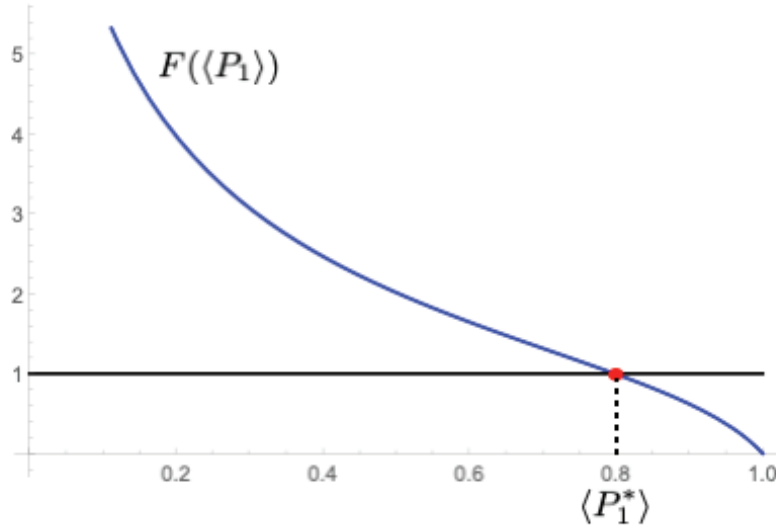


Figure 2.6: Solving Eq. (2.2.25) graphically in which the black line shows the line  $y = 1$  and the blue curve is the graph of the function  $F(\langle P_1 \rangle)$  when  $g(r) = 1$ .

Figure 2.6 illustrates an example of the function  $F$  against averaged singlet probability  $\langle P_1 \rangle$  in which  $F(0) > 1$ . The graph indicates that the equilibrium averaged singlet probability  $\langle P_1 \rangle$  can be solved uniquely. Thus, when  $F(0) > 1$ , there exists a unique solution  $\langle P_1 \rangle > 0$  but this could be solved only numerically.

From the Eq. (2.2.26), we can say that  $F(\langle P_1 \rangle)$  is a monotonically decreasing function of  $\langle P_1 \rangle$  that involves the summation of colonization for all pairs 0-1 and 1-0 and hence the pair correlation function  $g(r)$ .

For  $p = 0$ , the derived equilibrium pair probabilities become identical to those in Hamada and Takasu (2019) [10].

A baseline point pattern (CSR, clumped, over-dispersed) has been configured with the pair correlation function  $g(r)$  that measures the abundance of pairs. Therefore, the realized abundance of the four types of pairs are given by multiplying the equilibrium pair probabilities with  $g(r)$ . Now we have solved equilibrium singlet and pair probabilities using the moment closure and some approximations. The accuracy of the approximations is tested by simulations in the next section.

# Chapter 3

## Results

In this chapter, we show and compare the results of simulation and analytically derived singlet and pair probabilities at equilibrium applying point process approach. The results are illustrated based on the colonization kernels which are Gaussian and Step function, and three type of base-line point patterns including CSR, clumped and over-dispersed point patterns.

### 3.1 Examples of the point pattern dynamics

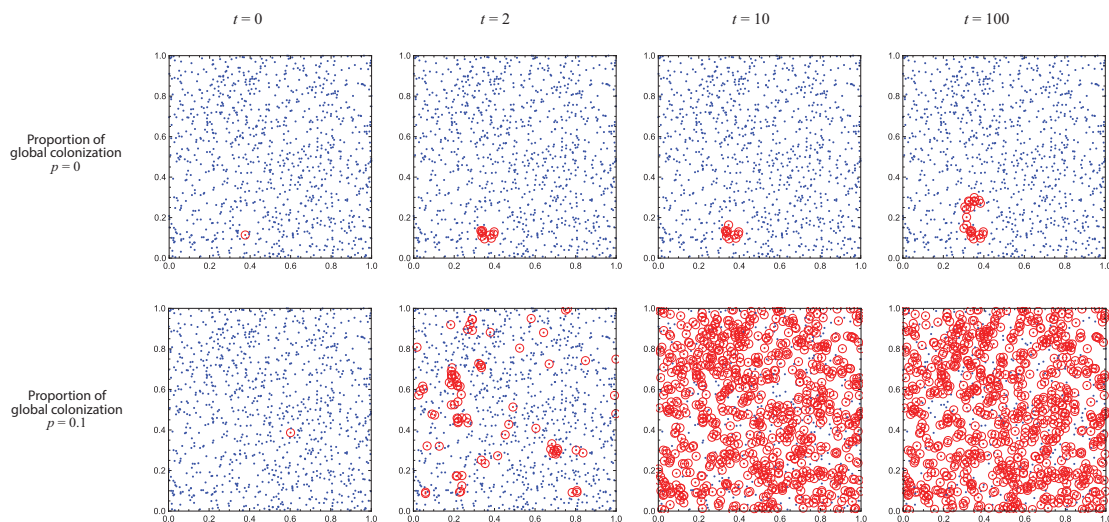


Figure 3.1: Temporal change of the point pattern on CSR ( $g(r) = 1$ ) with Gaussian kernel. Snapshots at  $t = 0, 2, 10, 100$  are shown from left to right column. The first row shows snapshots when there is only local colonization ( $p = 0$ ). The second row shows those when the proportion of global colonization  $p = 0.1$ . Empty patches are shown in blue, occupied patches are shown in red with radius  $2\sigma_c$  of the effective area of the local colonization kernel. Parameters are  $\sigma_c = 0.01, n = 1000, c_{l0} = c_g = 0.01, e = 1$ .

Figure 3.1 illustrates simulation examples on a CSR point pattern ( $g(r) = 1$ ) with Gaussian kernel. Without loss of generality, time  $t$  has been scaled so that the extinction rate is set  $e = 1$ . Initially, one randomly chosen patch is set occupied (red point). Occupied patches expand either by local or global colonization. Without global colonization ( $p = 0$ ), occupied patches expand only locally and very slowly because the range of local colonization is set small ( $\sigma_c = 0.01$ ). When we allow a small proportion of global colonization ( $p = 0.1$ ) with  $\sigma_c = 0.01$ , empty patches that are far away from occupied patches can be colonized and occupied patches spread over the entire space much faster than the case of  $p = 0$ .

Figure 3.2 shows dynamics of the proportion of empty and occupied patches as the 1st order structure of the point pattern. Starting from one occupied patch initially introduced, total extinction is possible by chance when all patches become empty in the stochastic point pattern dynamics. To explore the stochastic behaviors, we ran 100 realizations then calculated the average and standard deviation of the proportion of empty and occupied patches for realizations when total extinction does not occur. With the Gaussian kernel when there is no global colonization ( $p = 0$ ) and the range of local colonization is set small ( $\sigma_c = 0.01$ ), occupied patches are very slow to expand over space and variations among realizations are quite large compared with the cases with a larger range of local colonization  $\sigma_c = 0.02$  and/or a global colonization  $p = 0.1$ . Except the case with only local colonization ( $p = 0$ ) and small range of local colonization ( $\sigma_c = 0.01$ ), the proportion of empty and occupied patches nearly converges to the equilibrium mean-field singlet probabilities  $\langle P_0 \rangle$  and  $\langle P_1 \rangle$ , respectively. With the Step-function kernel for the case  $p = 0$  and  $\sigma_c = 0.01$ , occupied patches do not spread in almost all realizations because no local colonization is possible beyond  $2\sigma_c$ . For the case  $p = 0$  and  $\sigma_c = 0.02$ , occupied patches can spread but the proportion of occupied patches show a large variance among realizations because the location of an initially introduced occupied patch critically affects spatial expansion. Allowing global colonization  $p = 0.1$ , however, results in a good match with analytically derived equilibrium singlet probabilities.

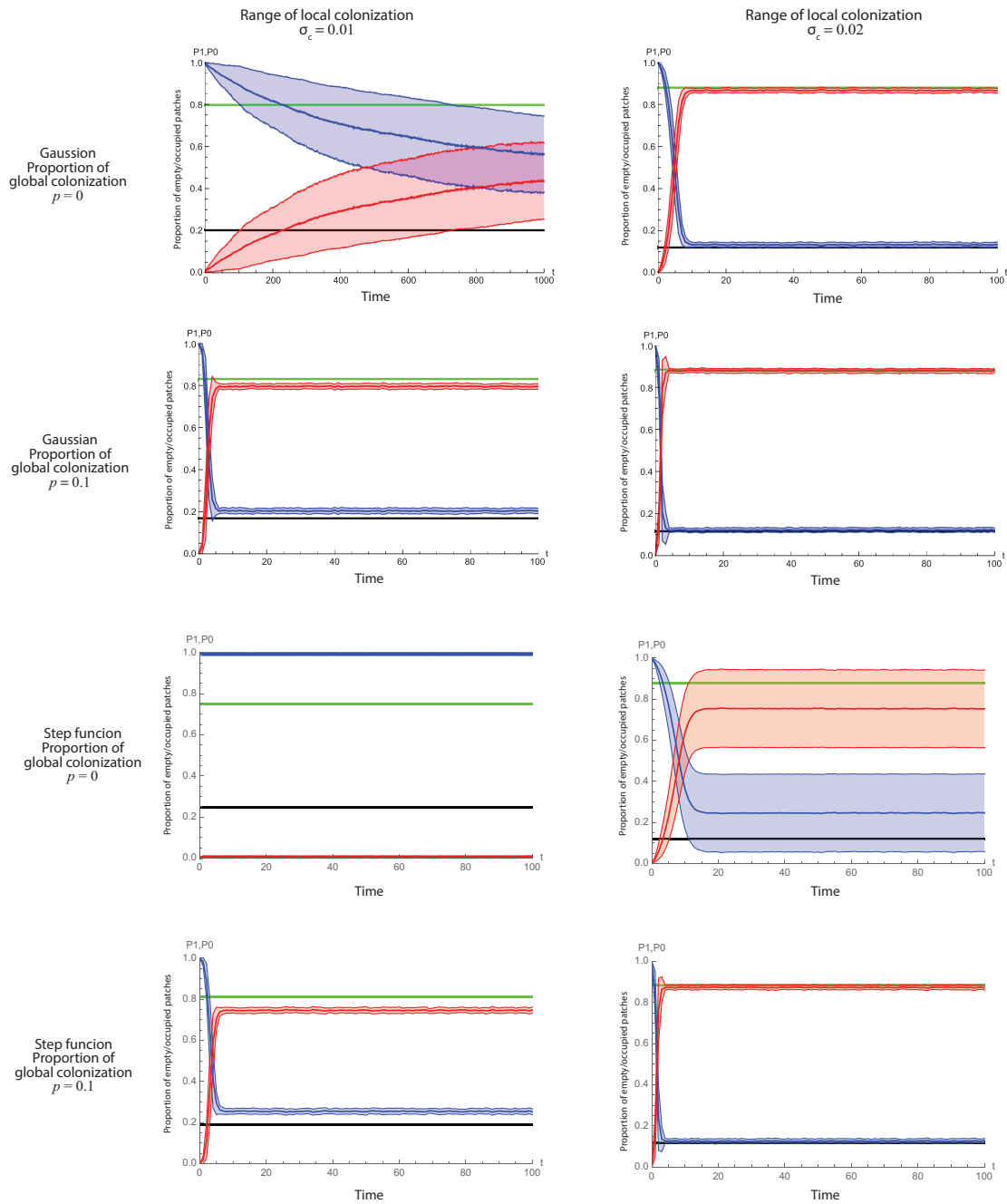


Figure 3.2: Temporal change of the proportions of empty and occupied patches on CSR with Gaussian and Step function kernel. Average and standard deviation are shown in thick solid curves and in shaded regions, respectively. Equilibrium mean-field singlet probability  $\langle P_0 \rangle$  and  $\langle P_1 \rangle$  is shown in green and black horizontal lines, respectively. The top two figures are for only local colonization  $p = 0$  and the bottom for a global colonization  $p = 0.1$ . The left and right column is  $\sigma_c = 0.01$  and  $\sigma_c = 0.02$ , respectively. Note the time span of the case of Gaussian kernel with  $p = 0$  and  $\sigma_c = 0.01$ . Other parameters are the same as in Figure 1:  $n = 1000, c_{l0} = c_g = 0.01, e = 1$ .

Figure 3.3 shows dynamics of the proportions of empty and occupied patches as the 1st order structure of the clumped point pattern with Gaussian and Step function kernels. We ran 100 realizations and calculated the average and standard deviation of the proportion of empty and occupied patches for realizations when total extinction does not occur. In the case of Gaussian kernel, when there is no global colonization ( $p = 0$ ) and the range of local colonization is set small ( $\sigma_c = 0.01$ ), occupied patches are slow to expand over space. The variation among the realizations for that case is large compared with the cases with a larger range of local colonization  $\sigma_c = 0.02$  and/or a global colonization  $p = 0.1$ . Except the case with only local colonization ( $p = 0$ ) and small range of local colonization ( $\sigma_c = 0.01$ ), the proportion of empty and occupied patches nearly converges to the equilibrium mean-field singlet probabilities  $\langle P_0 \rangle$  and  $\langle P_1 \rangle$ , respectively. Contrary in the case of Step function kernel, when there is only local colonization ( $p = 0$ ) the simulation results and derived analytical equilibrium results are totally different in both cases of  $\sigma_c = 0.01$  and  $\sigma_c = 0.02$ . For  $p = 0$  and  $\sigma_c = 0.01$ , occupied patches do not spread at all. This is because the range of local colonization is too small so that occupied patches do not spread to empty patches in neighbors. For  $p = 0$  and  $\sigma_c = 0.02$ , variation among realizations is very high. This is because occupied patches do not spread at all in some realizations if an initially introduced one occupied patch has no empty patches around it within  $2\sigma_c$ , but occupied patches spread if the initial occupied patch has empty patches within  $2\sigma_c$ . Introduction of a small proportion of global colonization  $p = 0.1$  results in a better match between simulation results and the analytically derived equilibrium.

Figure 3.4 demonstrates the dynamics of the proportions of empty and occupied patches as the 1st order structure on the over-dispersed point pattern with Gaussian and Step function kernels. For the Gaussian kernel, occupied patches expand over space more slowly compared with the case on the clumped point pattern. For the Step-function kernel, occupied patches do not spread at all. On the over-dispersed point pattern, points are spatially configured similar to regular lattice, i.e., there exists few short-distanced pairs and points tend to be separated. This leads to slower expansion under the Gaussian kernel and no expansion under the Step function kernel. However, if we allow global colonization or increase the range of local colonization  $\sigma_c$ , occupied patches expand over space and simulation results agree well with the analytically derived equilibrium.

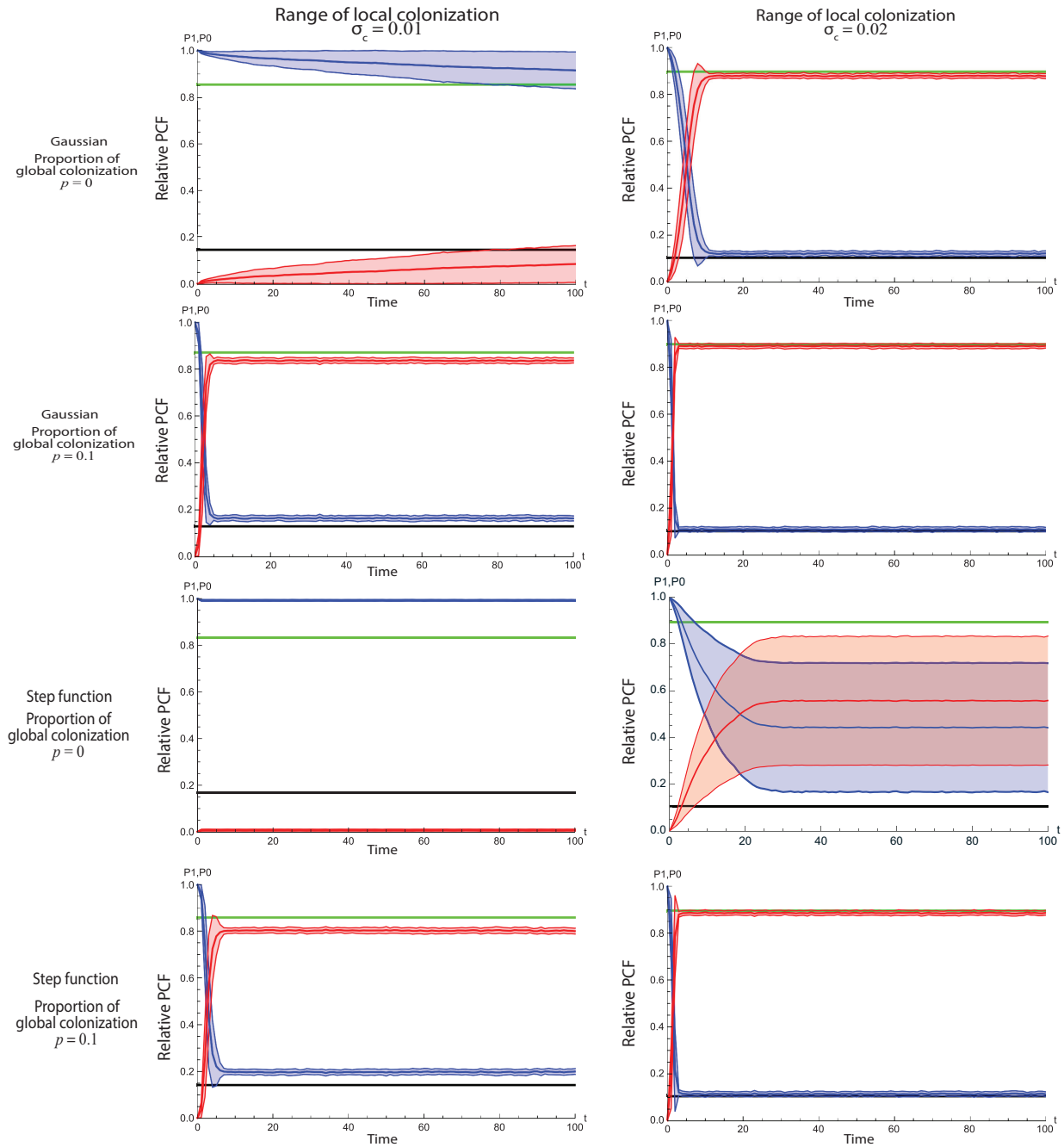


Figure 3.3: Temporal change of the proportions of empty and occupied patches on a clumped point pattern with Gaussian kernel and Step function kernel. The clumped point pattern has the pair correlation function  $g(r) = 1 + ae^{-br}$  with  $a = 1, b = 80$ . Average and standard deviation are shown in thick solid curves and in shaded regions, respectively. Equilibrium mean-field singlet probabilities  $\langle P_0 \rangle$  and  $\langle P_1 \rangle$  are shown in green and black horizontal lines, respectively. The top four figures are for the Gaussian kernel and the bottom for the Step function kernel. The left and right column is  $\sigma_c = 0.01$  and  $\sigma_c = 0.02$ , respectively.

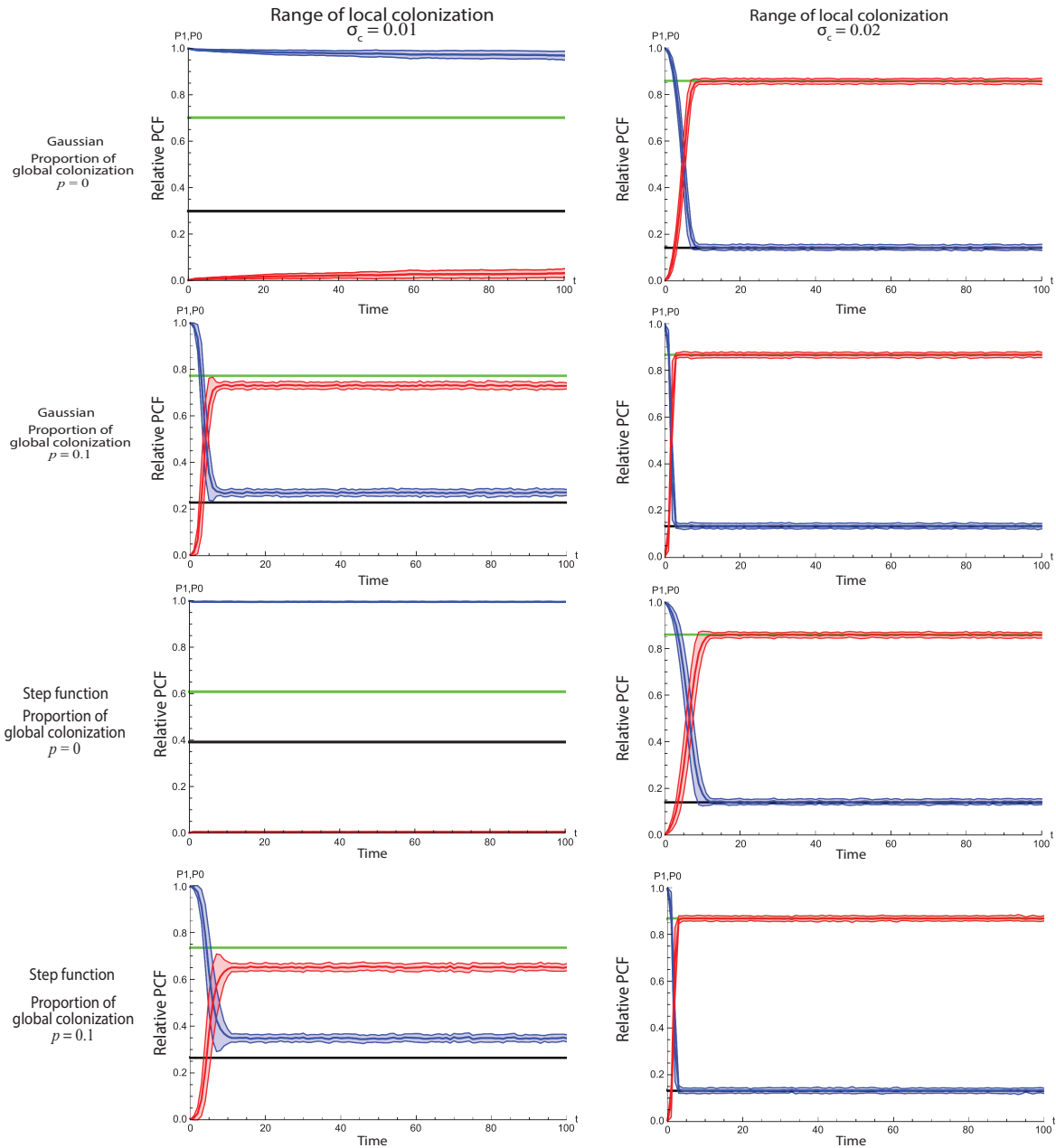


Figure 3.4: Temporal change of the proportions of empty and occupied patches on an over-dispersed point pattern with Gaussian kernel and Step function kernel. The over-dispersed point pattern has the pair correlation function  $g(r) = 1 + ae^{-br}$  with  $a = -1, b = 80$ . Average and standard deviation is shown in thick solid curves and in shaded regions, respectively. Equilibrium mean-field singlet probabilities  $\langle P_0 \rangle$  and  $\langle P_1 \rangle$  are shown in green and black horizontal lines, respectively. The top four figures are for the Gaussian kernel and the bottom for the Step function kernel. The left and right column is  $\sigma_c = 0.01$  and  $\sigma_c = 0.02$ , respectively.

Figure 3.5 demonstrates the relative pair correlation functions obtained in simulations and the equilibrium pair abundances that have been analytically derived on CSR point pattern with Gaussian kernel and Step function kernel. We ran 100 realizations then calculated average and standard deviation of each of the three relative pair correlation functions for realizations when total extinction does not occur. With the Gaussian kernel for the case with  $p = 0$  and  $\sigma_c = 0.01$ , occupied patches do not spread over the entire space in many realizations and variation among realizations is quite large. Simulation results are very different from the analytically derived pair abundances. However, we see that occupied patches tend to be locally clustered and that occupied and empty patches tend to separate each other because the pair correlation function becomes larger for the short distanced 1-1 pairs. On the other hand, empty and occupied patches tend to be separated because pair correlation function for 0-1 (1-0) pairs becomes smaller for the short distance. For other cases with  $p = 0.1$  or  $\sigma_c = 0.02$ , variation among realizations is small and this tendency becomes clearer. All of the relative pair correlation functions are both qualitatively and quantitatively similar to the equilibrium pair abundances analytically derived from the singlet and the pair dynamics for the cases with  $p = 0.1$  or  $\sigma_c = 0.02$ . With the Step function kernel, except the case with  $p = 0$  and  $\sigma_c = 0.01$  in which occupied patches do not spread at all in most realizations, occupied patches tend to be spatially clustered. However, this tendency becomes less clear if we allow a global colonization  $p = 0.1$  compared with the cases of the Gaussian kernel (cf. two figures for  $p = 0.1$  and  $\sigma_c = 0.02$ ). Analytically derived equilibrium pair abundances qualitatively match with the relative pair correlation functions obtained in simulation.

Figure 3.6 illustrates the relative pair correlation functions obtained in simulations on the clumped point pattern and the analytically derived equilibrium pair abundances with Gaussian kernel and Step function kernel. We ran 100 realizations and calculated the average and standard deviation of the three relative pair correlation functions for realizations when total extinction does not occur. With the Gaussian kernel, for the case with  $p = 0$  and  $\sigma_c = 0.01$ , occupied patches do not spread over the entire space and variation among realizations is large. Although simulation results are very different from the analytically derived relative pair correlation functions, we see that occupied patches tend to be locally clustered while occupied and empty patches tend to separate each other. For  $p = 0.1$  or  $\sigma_c = 0.02$ , simulation results match well with the analytically derived relative pair correlation functions. When  $p = 0$  in the case of the Step function kernel, occupied patches do not spread at all for  $\sigma_c = 0.01$  but they spread for  $\sigma_c = 0.02$ . Although simulation results and analytically derived relative pair correlation function do not match, occupied patches tend to be locally clustered with the same spatial scale. If we allow global colonization  $p = 0.1$ , simulations and analytical derivations agree well.

Figure 3.7 illustrates the relative pair correlation functions obtained in simulations on the over-dispersed point pattern and the analytically derived equilibrium pair abundances with Gaussian kernel and Step function kernel. As in the results on the clumped point pattern, the case  $p = 0$  and  $\sigma_c = 0.01$  results in a large difference between simulation results and analytically derived relative pair correlation functions. But for cases with  $p = 0.1$  or  $\sigma_c = 0.02$ , simulation results and the analytically derived relative pair correlation functions agree well.

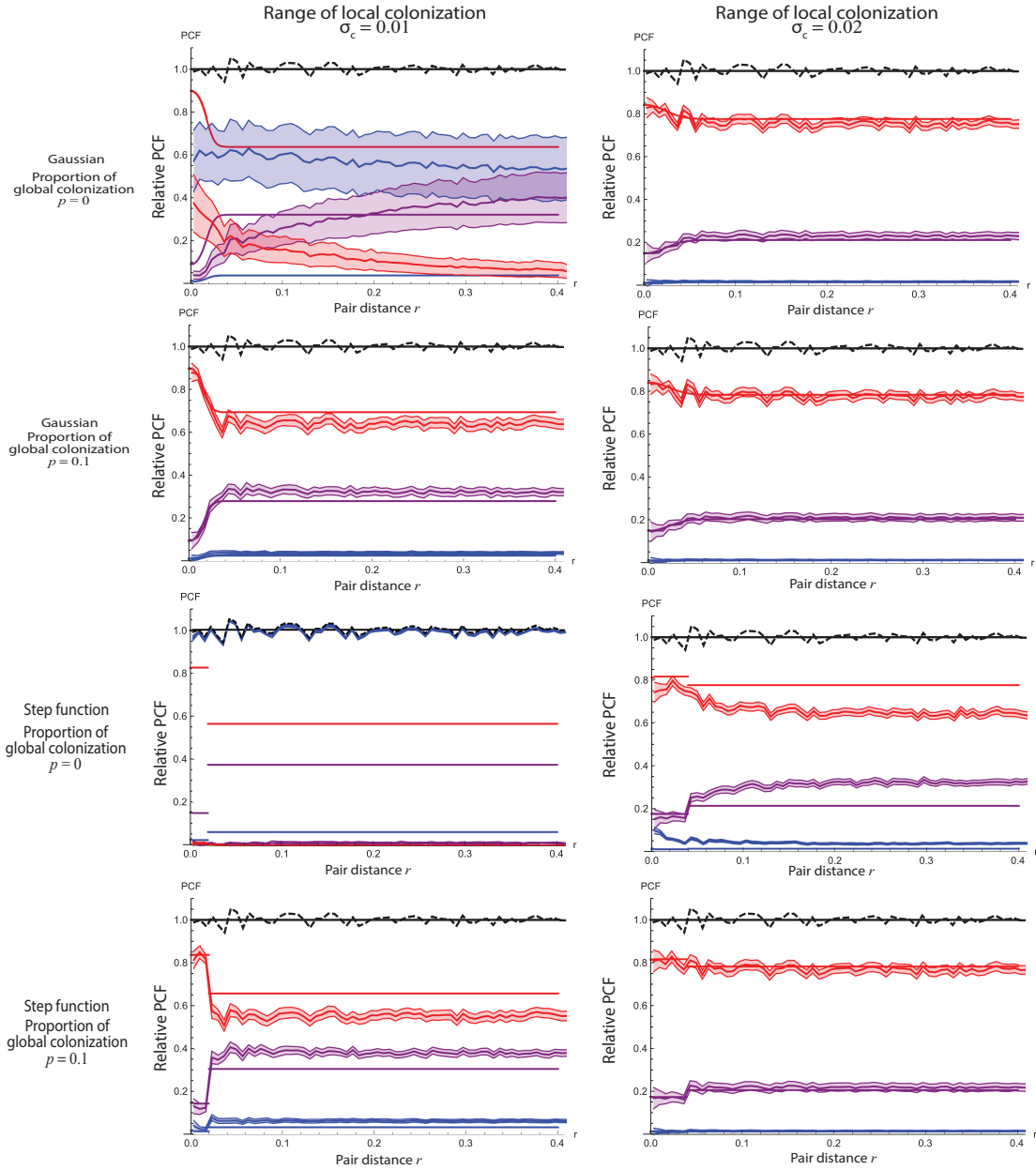


Figure 3.5: The relative pair correlation functions (PCF) on CSR with Gaussian and Step function kernel, at the final state of the simulation as functions of pair distance  $r$ . PCF with pairs 1-1, 0-1 (1-0), and 0-0 are shown in red, purple and blue, respectively. Sum of the four relative pair correlation functions is shown in black dash. The equilibrium pair abundance  $P_{11}(r)g(r), P_{01}(r)g(r) + P_{10}(r)g(r), P_{00}(r)g(r)$  derived from the singlet and pair dynamics are shown in solid line. Parameter values: Proportion of global colonization  $p = 0$  in the first and  $p = 0.1$  in the second row,  $\sigma_c = 0.01$  in the left and  $\sigma_c = 0.02$  in the right column.  $n = 1000, c_{l0} = c_g = 0.01, e = 1$ .

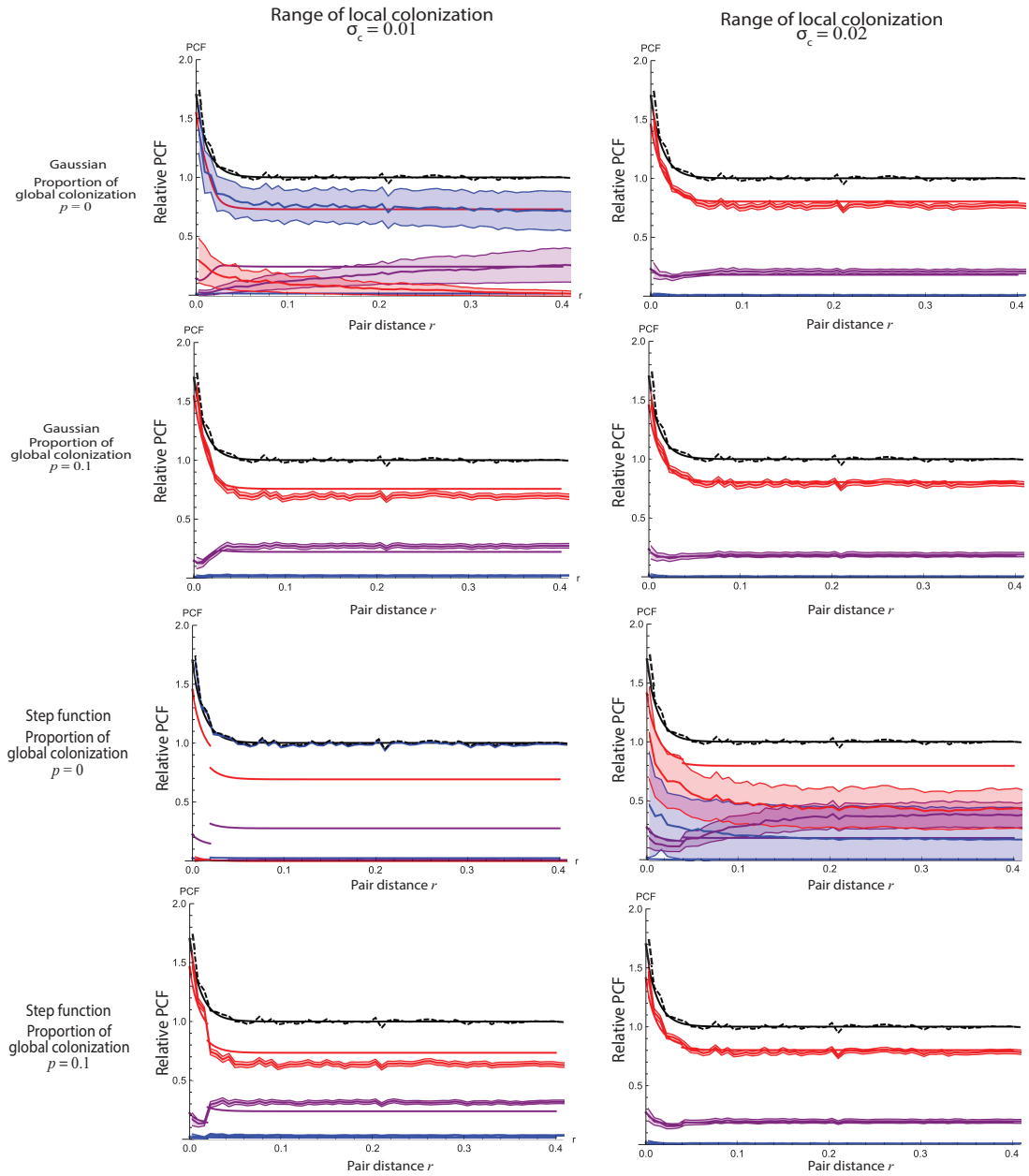


Figure 3.6: The relative pair correlation function (PCF) on a clumped point pattern with Gaussian kernel and Step function kernel, at the final state of the simulation as functions of pair distance  $r$ . Pair 1-1, 0-1 (1-0), and 0-0 are shown in red, purple and blue, respectively. Sum of the four relative pair correlation functions is shown in black dash. The equilibrium pair abundances  $P_{11}(r)g(r), P_{01}(r)g(r) + P_{10}(r)g(r), P_{00}(r)g(r)$  derived from the singlet and pair dynamics are shown in solid line. Parameter values: Proportion of global colonization  $p = 0$  in the first and  $p = 0.1$  in the second row,  $\sigma_c = 0.01$  in the left and  $\sigma_c = 0.02$  in the right column.  $N = 1000, c_{10} = c_g = 0.01, e = 1$ .

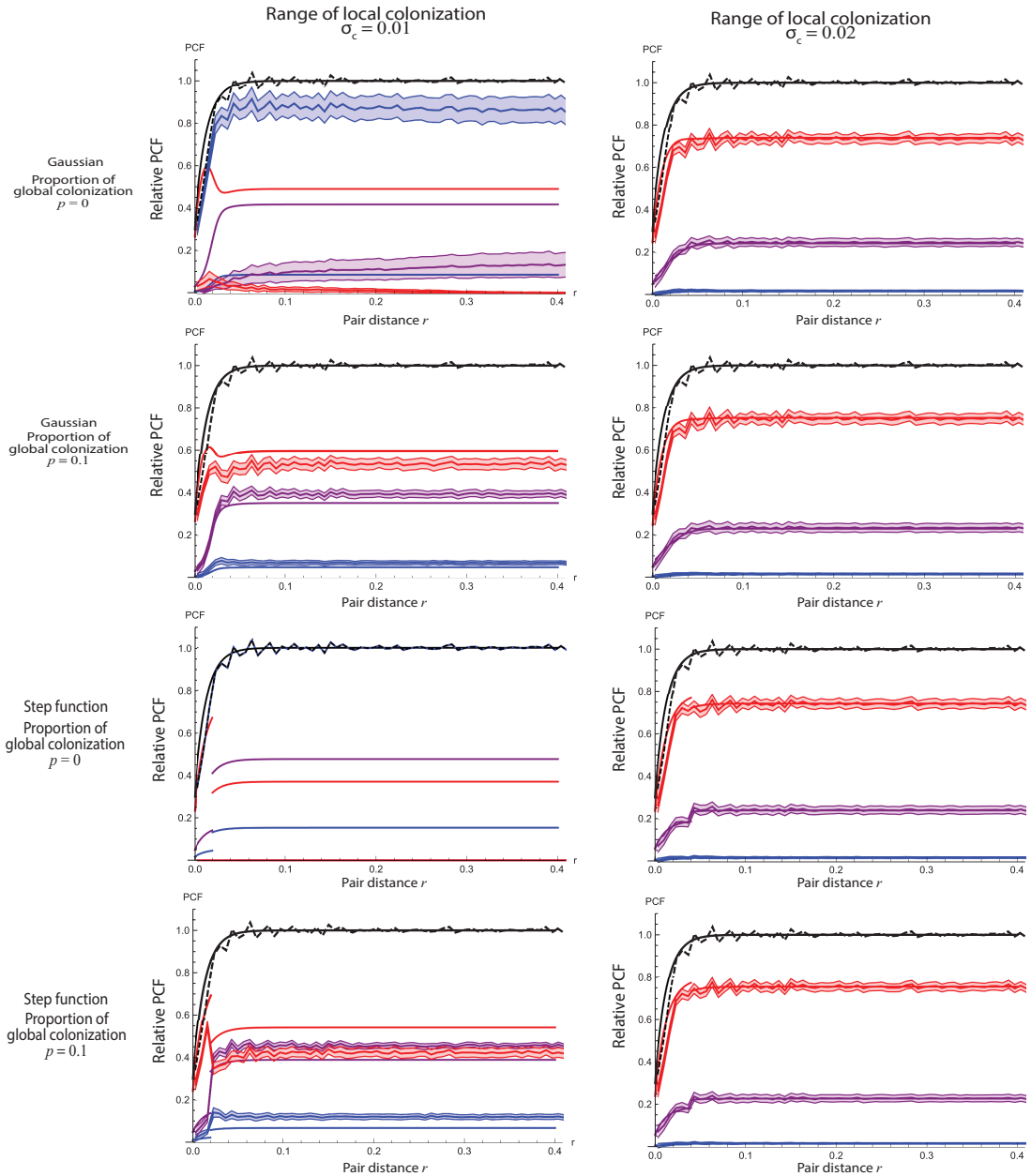


Figure 3.7: The relative pair correlation function (PCF) on an over-dispersed point pattern with Gaussian kernel and Step function kernel, at the final state of the simulation as functions of pair distance  $r$ . Pair 1-1, 0-1 (1-0), and 0-0 are shown in red, purple and blue, respectively. Sum of the four relative pair correlation functions is shown in black dash. The equilibrium pair abundance  $P_{11}(r)g(r), P_{01}(r)g(r) + P_{10}(r)g(r), P_{00}(r)g(r)$  derived from the singlet and pair dynamics are shown in solid line. Parameter values: Proportion of global colonization  $p = 0$  in the first and  $p = 0.1$  in the second row,  $\sigma_c = 0.01$  in the left and  $\sigma_c = 0.02$  in the right column.  $N = 1000, c_{10} = c_g = 0.01, e = 1$ .

### 3.2 Dependency of the 1st order equilibrium on parameters

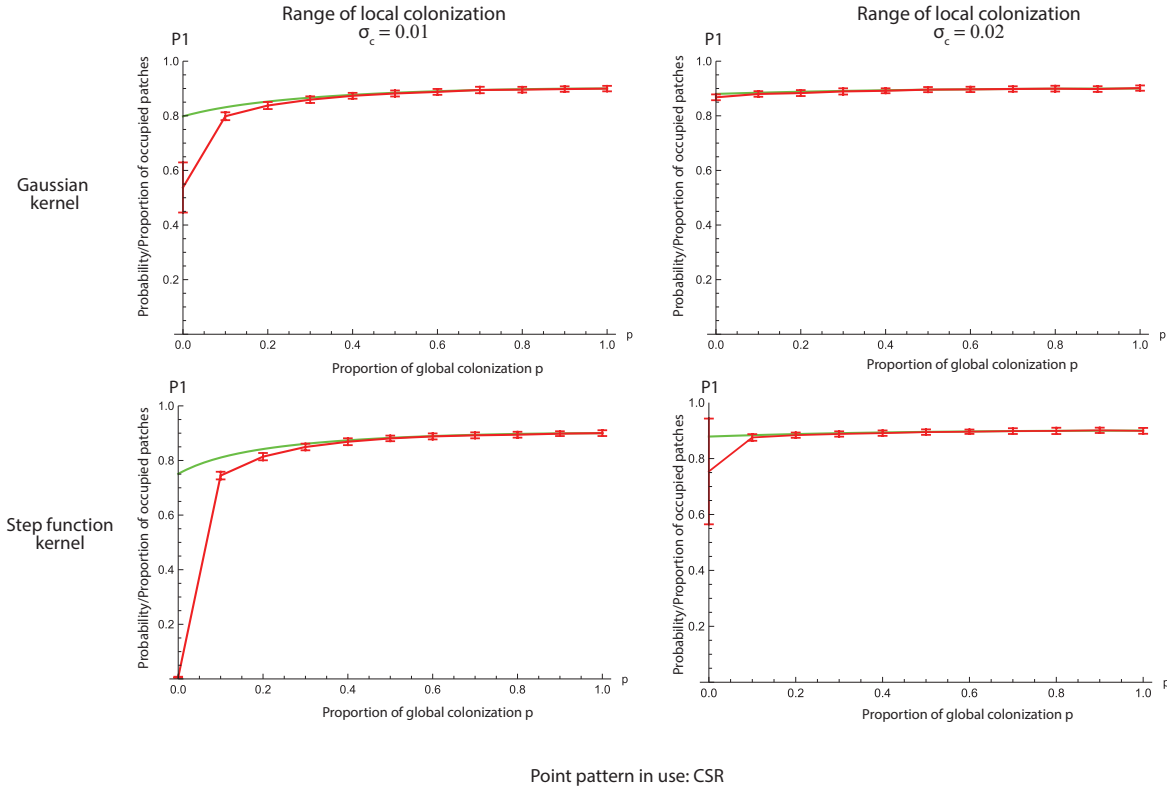


Figure 3.8: Dependency of the proportion of occupied patches on the proportion of global colonization  $p$  on CSR point pattern. Analytically derived equilibrium singlet probability  $\langle P_1 \rangle$  is shown in green, and simulation results (average  $\pm$  standard deviation for 100 realizations) is shown in red. The top two figures are for the Gaussian kernel, while the bottom ones are for the Step function kernel. The left and right column is  $\sigma_c = 0.01$  and  $\sigma_c = 0.02$ , respectively.  $n = 1000, c_{l0} = c_g = 0.01, e = 1$ .

Figure 3.8 plots the equilibrium proportion of occupied patches as the 1st order structure against the proportion of global colonization rate  $p$  on CSR point pattern. Simulation results as the average proportion of occupied patches for 100 realizations when total extinction does not occur and analytically derived average singlet probability  $\langle P_1 \rangle$  are compared. When the range of local colonization is large ( $\sigma_c = 0.02$ ), proportion of occupied patches and the analytically derived equilibrium singlet probability  $\langle P_1 \rangle$  agree very well with each other except for  $p \ll 1$  and  $p$  does not affect both. However, when the range of local colonization is small ( $\sigma_c = 0.01$ ), simulation results become smaller than the analytically derived equilibrium. Without global colonization  $p = 0$ , occupied patches do not spread in nearly all realizations for the Step function kernel. The same result as Hamada and Takasu (2019) [10] showed. The model in the case  $p = 1$  corresponds to the non-spatial Levins model and the proportion of occupied patches  $\langle P_1 \rangle$  is 0.9 from Eq. (1.2.2).

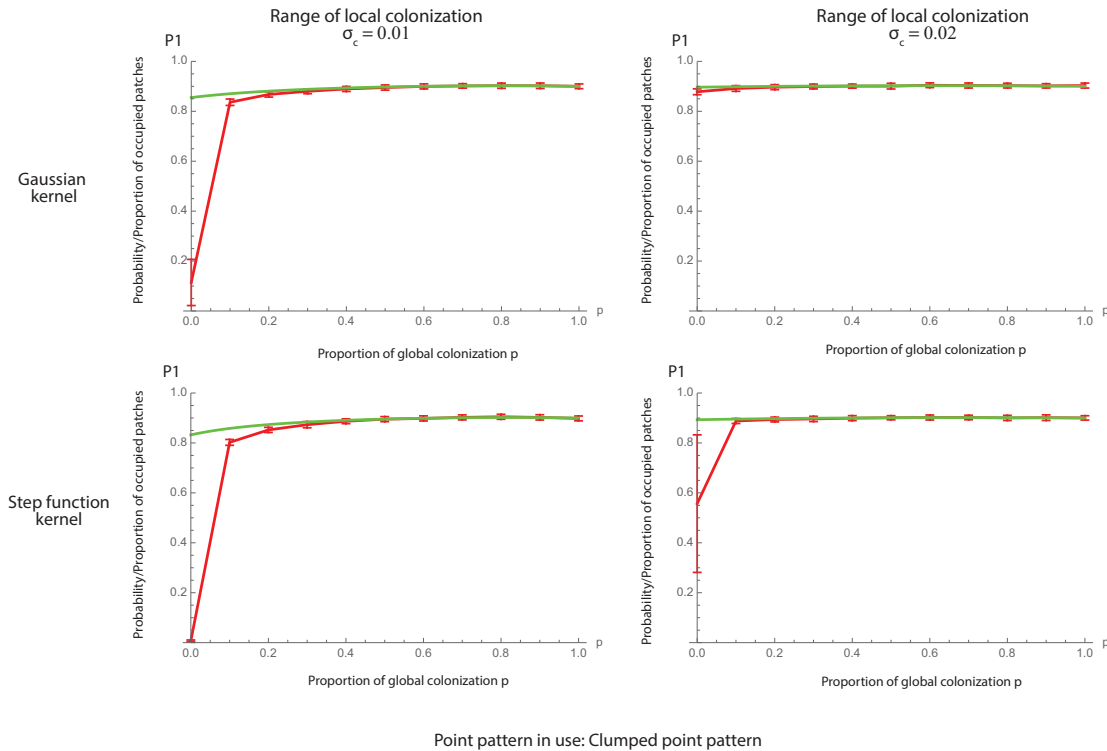


Figure 3.9: Dependency of the proportion of occupied patches on the proportion of global colonization  $p$  on clumped point pattern. Analytically derived equilibrium singlet probability  $\langle P_1 \rangle$  is shown in green, and simulation results (average  $\pm$  standard deviation for 100 realizations) is shown in red. The top two figures are for the Gaussian kernel, while the bottom ones are for the Step function kernel. The left and right column is  $\sigma_c = 0.01$  and  $\sigma_c = 0.02$ , respectively.  $n = 1000, c_{l0} = c_g = 0.01, e = 1$ .

Figures 3.9 and 3.10 plot the equilibrium proportion of occupied patches as the 1st order structure against the proportion of global colonization  $p$  on clumped and over-dispersed point pattern, respectively. Simulation results as the average proportion of occupied patches for 100 realizations when total extinction does not occur and analytically derived average singlet probability  $\langle P_1 \rangle$  are compared. When  $\sigma_c = 0.01$ , simulation results become very smaller than  $\langle P_1 \rangle$  for small  $p$  both for the Gaussian and the Step-function kernel and on clumped and over-dispersed point pattern. When  $\sigma_c = 0.02$ , simulation results and  $\langle P_1 \rangle$  agree very well with each other both for the two kernels when  $p$  is not small (e.g.,  $p \geq 0.1$ ). Note that they agree very well even for  $p = 0$  for the Step-function kernel on over-dispersed point pattern.

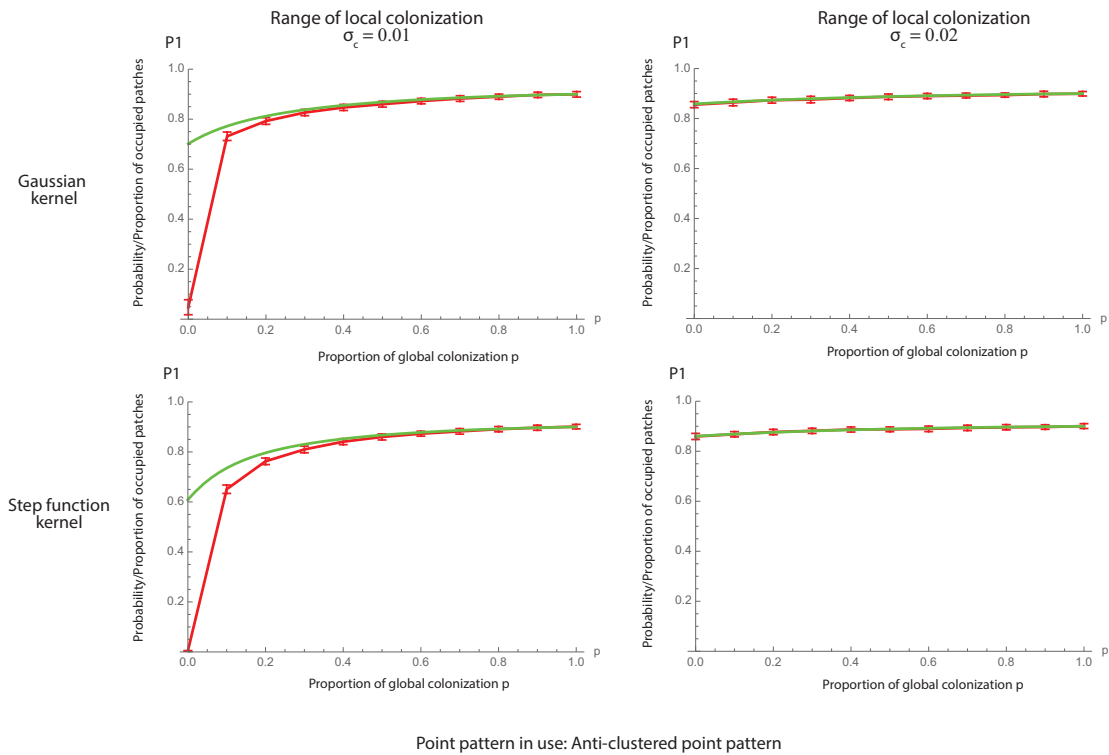


Figure 3.10: Dependency of the proportion of occupied patches on the proportion of global colonization  $p$  on over-dispersed point pattern. Analytically derived equilibrium singlet probability  $\langle P_1 \rangle$  is shown in green, and simulation results (average  $\pm$  standard deviation for 100 realizations) is shown in red. The top two figures are for the Gaussian kernel, while the bottom ones are for the Step function kernel. The left and right column is  $\sigma_c = 0.01$  and  $\sigma_c = 0.02$ , respectively.  $n = 1000, c_{l0} = c_g = 0.01, e = 1$ .

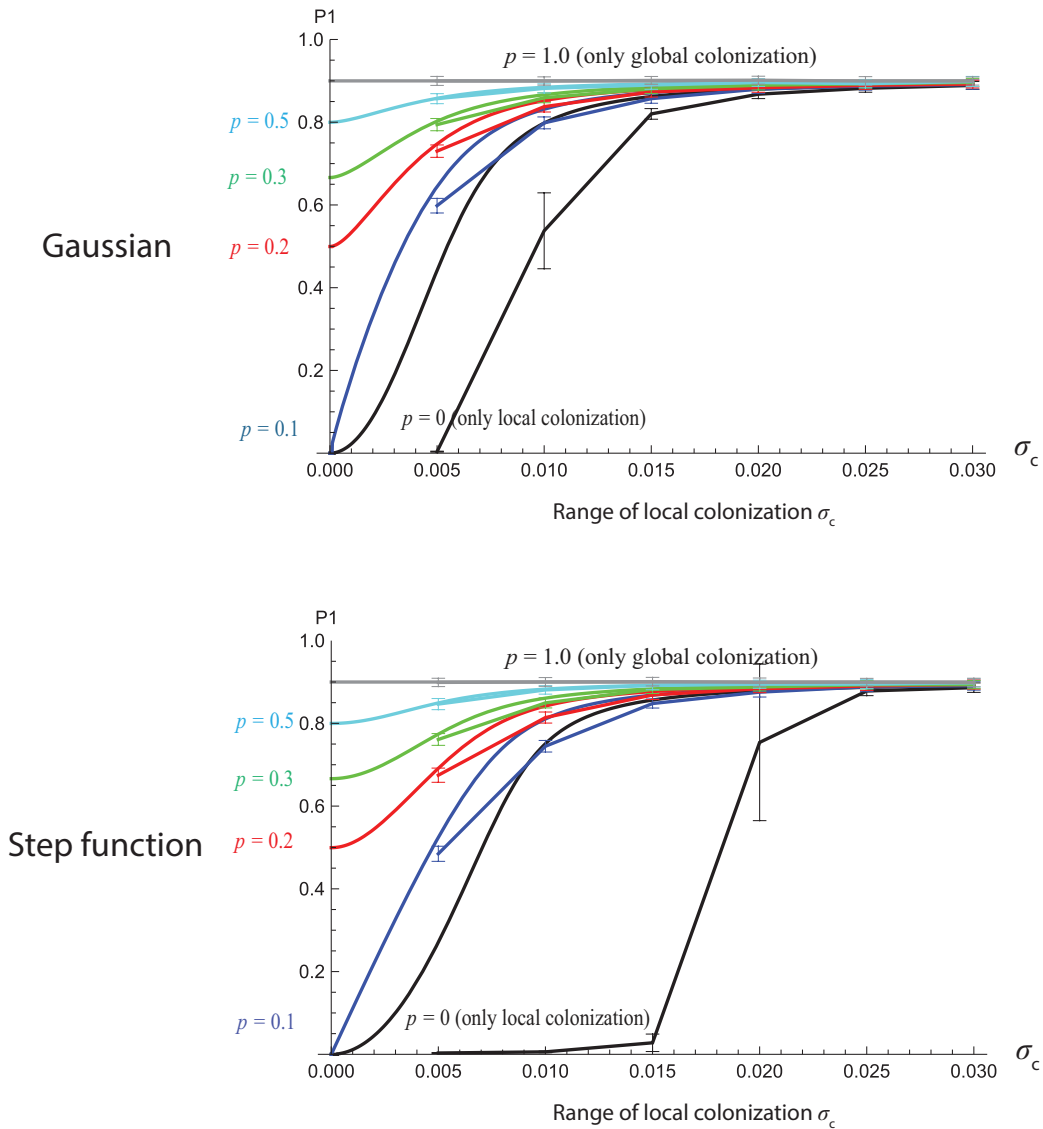


Figure 3.11: Dependency of the proportion of occupied patches on the proportion of local colonization range  $\sigma_c$  on CSR point pattern for a range of global colonization proportion  $p$ . Analytically derived singlet probability  $\langle P_1 \rangle$  is shown in the smooth curve, and simulation results are shown with average  $\pm$  standard deviation for 100 realizations when total extinction did not occur.  $n = 1000, c_{l0} = c_g = 0.01, e = 1$ .

Figure 3.11 plots the equilibrium proportion of occupied patches but against the range of local colonization  $\sigma_c$  on CSR point pattern. Simulation results as the average proportion of occupied patches for 100 realizations when total extinction does not occur and analytically derived average singlet probability  $\langle P_1 \rangle$  are compared. When there is only local colonization ( $p = 0$ ), simulation results deviate most from  $\langle P_1 \rangle$ . As  $p$  is increased, simulation results agree well with  $\langle P_1 \rangle$  and agreement is better in Gaussian than Step function kernel. Again the same result as Hamada and Takasu (2019) [10] showed.

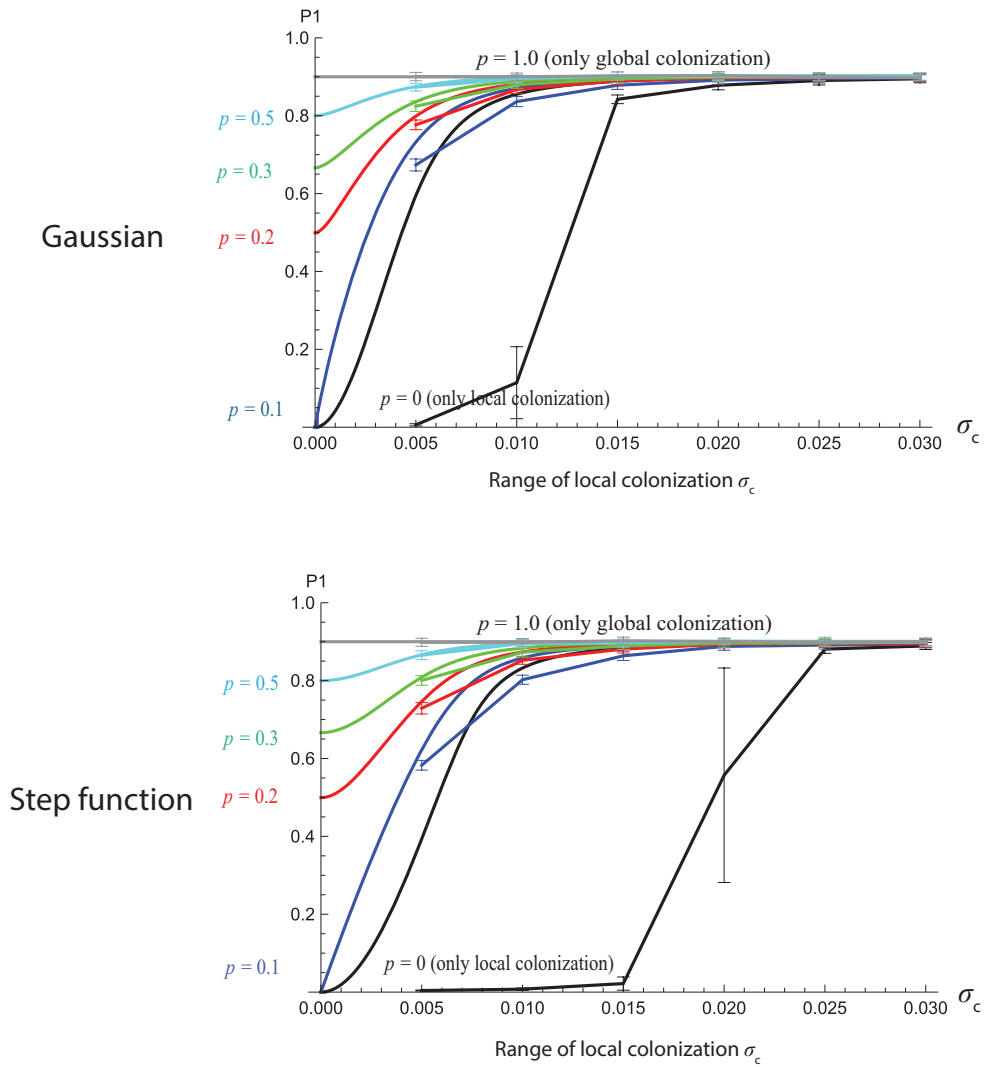


Figure 3.12: Dependency of the proportion of occupied patches on the proportion of local colonization range  $\sigma_c$  on a clumped point pattern for a range of global colonization proportion  $p$ . Analytically derived equilibrium singlet probability  $\langle P_1 \rangle$  is shown in the smooth curve, and simulation results are shown with average  $\pm$  standard deviation for 100 realizations when total extinction did not occur.  $n = 1000, c_{l0} = c_g = 0.01, e = 1$ .

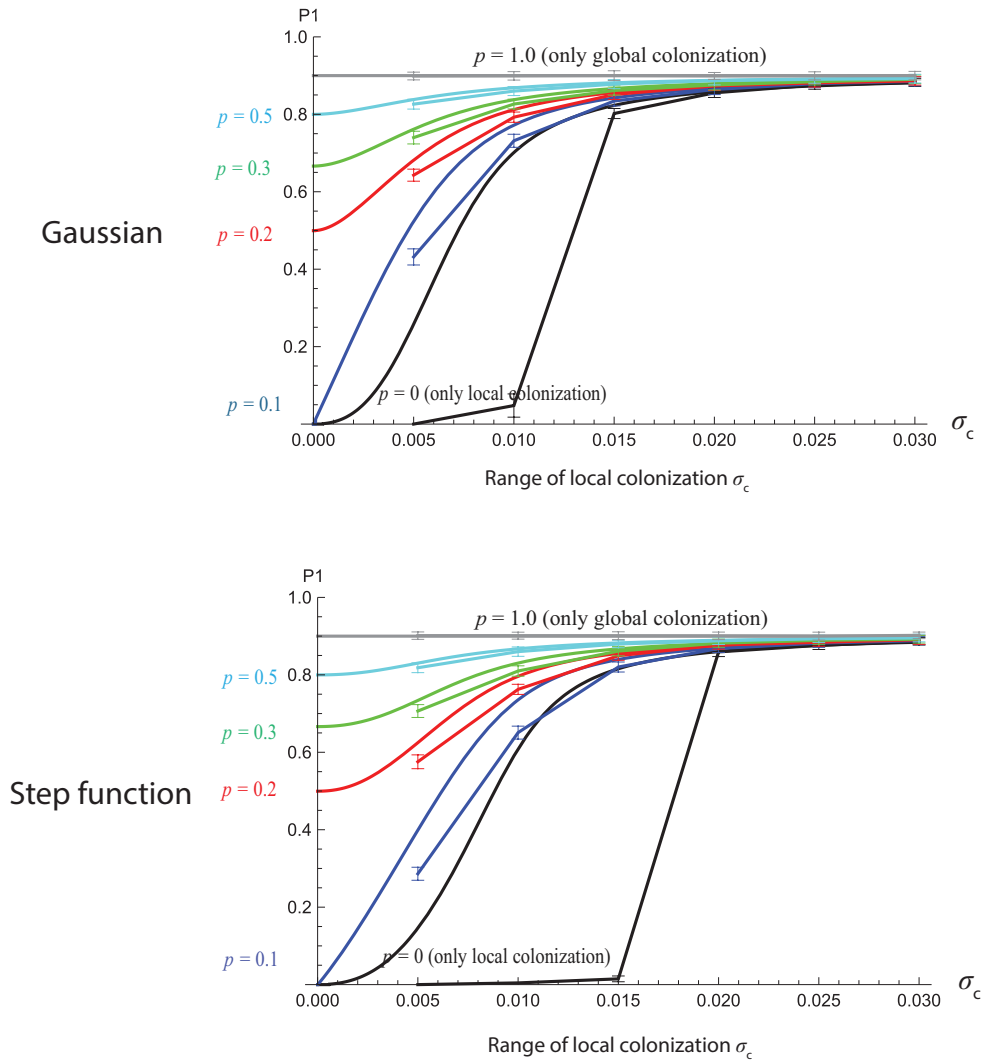


Figure 3.13: Dependency of the proportion of occupied patches on the proportion of local colonization range  $\sigma_c$  on an over-dispersed point pattern for a range of global colonization proportion  $p$ . Analytically derived equilibrium singlet probability  $\langle P_1 \rangle$  is shown in the smooth curve, and simulation results are shown with average  $\pm$  standard deviation for 100 realizations when total extinction did not occur.  $n = 1000, c_{l0} = c_g = 0.01, e = 1$ .

Figures 3.12 and 3.13 plot the equilibrium proportion of occupied patches but against the range of local colonization  $\sigma_c$  on the clumped and the over-dispersed point pattern. Simulation results of the proportion of occupied patches are averages of 100 realizations when total extinction does not occur and compared with analytically derived average singlet probability  $\langle P_1 \rangle$ . Sharing the same conclusion as the case of CSR point pattern, when there is only local colonization ( $p = 0$ ), simulation results deviate most from  $\langle P_1 \rangle$ . As  $p$  is increased, simulation results agree well with  $\langle P_1 \rangle$  and agreement is better in Gaussian than Step function kernel. Again the same result as Hamada and Takasu (2019) [10] showed.

### 3.3 Probability of total extinction

Total extinction is possible in our stochastic point pattern dynamics when all patches become empty. To explore the probability of total extinction, we ran 100 realizations starting from one occupied patch randomly introduced for a combination of local colonization range  $\sigma_c$  and global colonization proportion  $p$ . Probability of total extinction was calculated as the proportion of realizations that total extinction occurred. One can relate the extinction probability of a metapopulation to studies of the persistence of a metapopulation and metapopulation persistence time.

Figure 3.14 shows the probability of total extinction plotted against  $\sigma_c$  and  $p$  on CSR point pattern for Gaussian and Step function kernel. The probability of total extinction is significantly high when the range of local colonization is small and the proportion of global colonization is small as well. In general, the extinction probability in the case of the Step function kernel is greater than that of the Gaussian kernel. However, this tendency is not clear for large  $\sigma_c$  and  $p$ . Even for a large local colonization range and large proportion of global colonization, extinction probability is not close to zero.

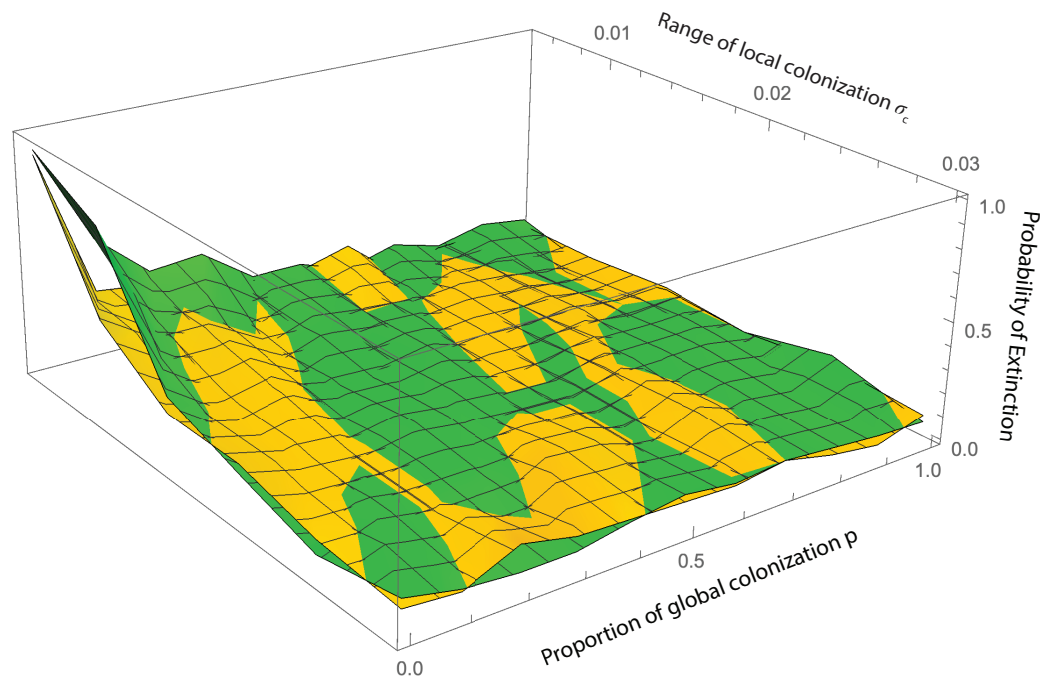


Figure 3.14: Probability of total extinction plotted against local colonization range  $\sigma_c$  and global colonization proportion  $p$  on CSR point pattern for Gaussian (yellow) and Step function (green) kernel.  $n = 1000, c_{l0} = c_g = 0.01, e = 1$

We have done the same analysis for clumped and over-dispersed baseline point patterns. A clumped point pattern was generated such that its pair correlation function is given by  $g(r) = 1 + ae^{-br}$  with  $a = 1, b = 80$ . Then we ran the stochastic simulation on it. In the same way, an over-dispersed point pattern was generated ( $a = -1, b = 80$ ), and simulations were done. Qualitatively the same results have been obtained. Introduction of a small proportion of global colonization results in fast convergence to the equilibrium state of the dynamics. With a large local colonization range, the analytically derived 1st order and 2nd order structure agree well with simulation results.

Finally, Figures 3.15 and 3.16 plot the probability of total extinction starting from one occupied patch for a combination of the range of local colonization  $\sigma_c$  and global colonization proportion  $p$  calculated from 100 realizations on the clumped and the over-dispersed point pattern, respectively. Both the figures are quite similar in shape to those of CSR (cf. Figure 3.14). The total extinction probability is higher in the case of Step-function than in that of Gaussian kernel for both types of point pattern. The total extinction probability is slightly higher in over-dispersed than in CSR and clumped point pattern when  $\sigma_c$  and  $p$  are small.

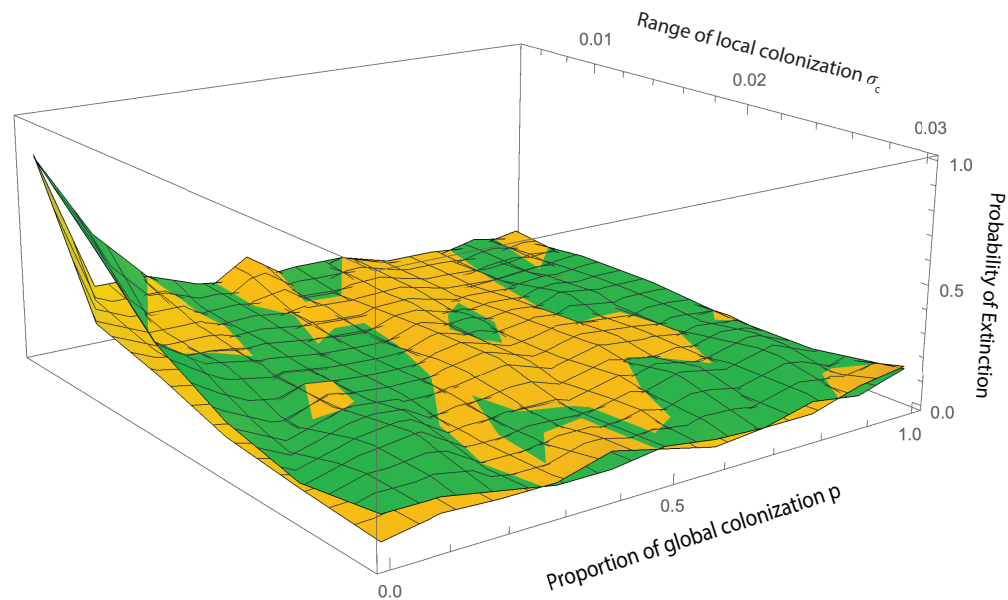


Figure 3.15: Probability of total extinction plotted against local colonization range  $\sigma_c$  and global colonization proportion  $p$  on a clumped point pattern for Gaussian (yellow) and Step function (green) kernel.  $n = 1000, c_{l0} = c_g = 0.01, e = 1$

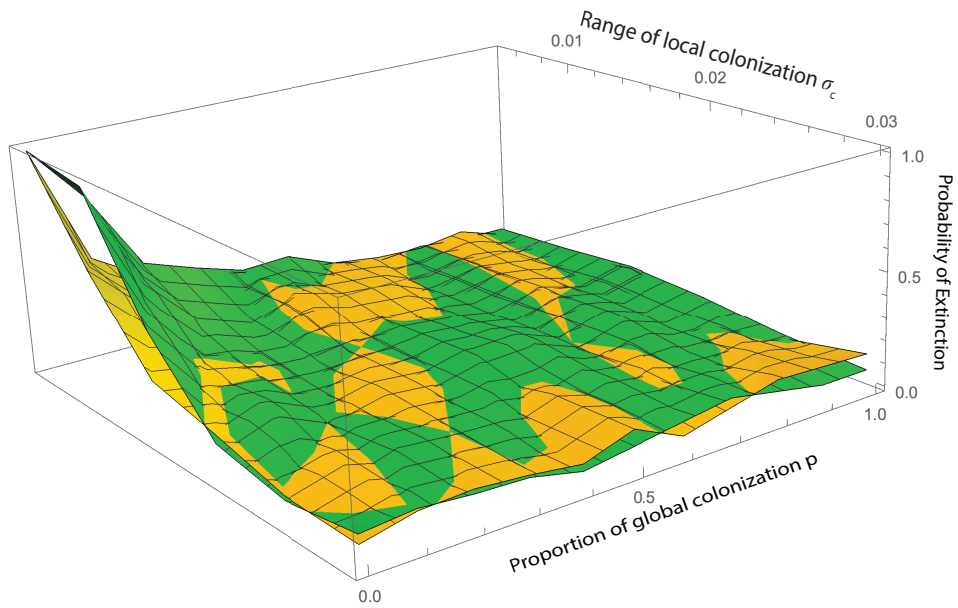


Figure 3.16: Probability of total extinction plotted against local colonization range  $\sigma_c$  and global colonization proportion  $p$  on an over-dispersed point pattern for Gaussian (yellow) and Step function (green) kernel.  $n = 1000, c_l = c_g = 0.01, e = 1$

# Chapter 4

## Discussion

We have implemented a spatial metapopulation model as a stochastic point pattern dynamics. Local patches are spatially distributed with a certain configuration in which an empty patch is occupied by colonization including both local and global colonization and an occupied patch becomes empty by local extinction. The point pattern eventually converges to an equilibrium state. We also have derived an analytical model in terms of singlet and pair probabilities that we expect will capture the essence of the stochastic point pattern dynamics. The derived analytical model connects the classical Levins model and our spatially explicit metapopulation model by the proportion of global colonization rate  $p$ . Using simple closures to approximate triplet probabilities, we have successfully derived equilibrium singlet and pair probabilities analytically, and then compared simulation and analytical results.

Generally, the analytically derived equilibrium properties successfully describe simulation results for two colonization kernels tested and three types of baseline point pattern on which the stochastic dynamics runs when the range of local colonization  $\sigma_c$  is large and the proportion of global colonization  $p$  is not too small. Introduction of a small proportion of global colonization leads to a quick convergence to an equilibrium state of the point pattern. The derived equilibrium properties, however, become poor to describe simulations as the local colonization range  $\sigma_c$  becomes smaller when  $p$  is near zero. In such cases, an empty patch and a cluster of local patches is nearly isolated from other patches and clusters in the landscape, respectively, and local colonization among patches and clusters is very unlikely to occur. Therefore, when  $\sigma_c$  is small and  $p = 0$ , we cannot convince that the proportion of occupied patches converges to the equilibrium mean-field singlet probability analytically derived (Figure 3.2 for  $\sigma_c = 0.01$ ,  $p = 0$ ). Success of the analytically derived equilibrium compared with simulations critically depends on the degree of connectedness of local patches. This also relates to the extinction probability. For small  $\sigma_c$  and  $p \approx 0$ , the effective area  $A = 4\pi\sigma_c^2$  of a local patch does not overlap with that of other patch(es) and thus chance of extinction, starting from one occupied patch, becomes high. While there is a small chance of local colonization to an empty patch beyond the distance  $2\sigma_c$  in Gaussian kernel, local colonization beyond  $2\sigma_c$  is zero in Step-function kernel. This leads to the greater extinction probability in Step-function kernel than in Gaussian kernel for all of the three baseline point patterns used.

The approximation of mean-field value in the Eq. (2.2.14) could result in overestimation

when  $\sigma_c$  is small. This can be clearly seen in Figures 3.2 to 3.7 in the case when  $p = 0$  and  $\sigma_c = 0.01$ , the analytically derived singlet and pair probabilities significantly differ from simulation results, especially with Step function kernel for all three types of point pattern. When global colonization is included,  $p = 0.1$ , the overestimation of that approximation is reduced, as we can see the analytical results reach much closer to simulation results. When the range of local colonization is large enough, the approximation works well which can be seen in above-mentioned figures as  $\sigma_c = 0.02$ .

Moreover, although we have shown in our research that the analytically derived equilibrium singlet and pair probabilities could be uniquely solved, we do not mathematically check the stability of the solutions as well as how accurate the solutions are. These evaluations are beyond the scope of this research. Further study of these aspects could be worth exploring.

It is indisputable that the classical Levins metapopulation model is a valuable theoretical starting point. However, it still falls short of describing realistic metapopulations we observe in nature. To study more realistic and complex situations, various models have been explored. For example, Hanski (1983) [11] derived a mathematical model for two competing species which may or may not regionally coexist. After that, in [21] Hastings (1991) developed structured models of metapopulation dynamics that explicitly considered population size in patches and showed that two positive equilibria were possible. In the same year, Hanski incorporated local dynamics into metapopulation models and constructed a modified Levins model which takes into account the empirically observed negative relationship between extinction probability and the fraction of occupied patches ([13]). Whilst, Hanski and Gyllenberg (1993) [17] have had an alternative perspective on metapopulation models that allow for spatial variation in habitat patch size. North and Godfray (2017) [28] have developed a spatially explicit metapopulation model to study how host and pathogen dispersal jointly affect disease persistence.

There have been two major approaches to mathematically study point pattern dynamics in general; the method of moments and the method of perturbation expansion. In the method of moments, we derive dynamics of spatial moments as the mean-field density of points (1st order structure) and the correlation of pairs made by two points (2nd order structure) and triplets, etc., that are built up from mechanistic interactions among points. Except for trivial cases, however, the derived dynamics of hierarchical orders is not closed and the dynamics is mathematically intractable. To close the dynamics, we need to adopt ad hoc moment closure, thereby a higher order moment is approximated with a combination of lower order moments (Bolker (1999) [1], Dieckmann and Law (2000) [7], North and Godfray (2017) [28]). On the other hand, the method of perturbation expansion has been proposed as an alternative approach to explore point pattern dynamics. It does not require moment closure and can derive spatial moments of all orders that are exact in the limit when the interaction range is infinitely large (Ovaskainen and Cornell (2006a) [29], Ovaskainen and Cornell (2006b) [30], Cornell and Ovaskainen (2008) [4], Ovaskainen et al. (2014) [31], Cornell et al. (2019) [5]).

Spatial metapopulation dynamics has been studied as point pattern dynamics (or point process) over the past couple of decades. Ovaskainen and Cornell (2006a) [29] extended the classical Levins model as we have done in this paper but only local colonization was considered in their model. They developed a novel method of perturbation expansion around the mean-field dynamics in which ad hoc moment closure is not required and the proportion of occupied patches

and the spatial correlation at equilibrium are derived in a closed form. They showed that the patch occupancy can be increased or decreased by spatial structure of the baseline landscape. We obtain the same results; analytically derived proportion of occupied patches depends on the baseline landscape through the parameter  $a$  in the pair correlation function  $g(r)$  of the baseline landscape in Eq. (2.2.25) ( $a = 0$  for CSR,  $a > 0$  for clustered and  $a < 0$  for over-dispersed). This can be confirmed in Figures 3.8, 3.9 and 3.10 as well as Figures 3.11, 3.12 and 3.13.

Although Ovaskainen and Cornell (2006a) [29] analyzed the same metapopulation dynamics but only with local colonization being considered, mathematical formulation is slightly different from ours. In the derivation of stochastic dynamics of status  $P_i$  of the point  $i$  ( $P_i(t) \in \{0, 1\}$ ) as stochastic differential equation (SDE), status of the point  $i$  and  $j \neq i$  has been de-coupled and correlation between the point  $i$  and  $j$  has been removed (Eq. (3) of Ovaskainen and Cornell (2006a) [29]). But in our formulation, we keep the correlation using the pair probability  $P_{ij01}$  in the singlet dynamics. In many theoretical studies of metapopulation, this de-coupling seems to be a priori accepted. But in theoretical studies of epidemics, it is not, i.e.,  $P_{ij01} \neq P_{i0}P_{j1}$ . It remains not clear if this difference in mathematical formulation leads to fundamental differences in the analysis.

The method of perturbation expansion has been applied to various spatial dynamics and formalized more rigorously (Ovaskainen and Cornell (2006b) [30], Cornell and Ovaskainen (2008) [4], Ovaskainen et al. (2014) [31]). Cornell et al. (2019) [5] further applied the method of perturbation expansion to ecological interactions at individual-level in general and provided a unified framework for analysis of individual-based models. Moment closure used in this paper as the method of moments is easier to apply than the method of perturbation expansion. Although both the methods are fundamentally different in its origin, both may reflect two sides of the same coin; they may be essentially the same but they describe the target dynamics in different manners. Further research is needed to explore how both the methods are related to each other.

Combination of local and global colonization has been studied in a lattice-structured landscape using lattice model. Harada and Iwasa (1994) [19] studied the effect of vegetative production as local colonization to neighbor patches and seed production as global colonization to all empty patches in lattice space. Based on simulation and pair approximation analyses, they showed that there is an optimal fraction of local colonization that maximizes the density of occupied patches at equilibrium. Harada (1999) [18] further studied evolutionary dynamics of the allocation to local dispersers with a linear trade-off between local and global dispersers. In both studies, proportion of occupied patches is maximized at a certain combination of local and global dispersers. Our model also assumes a linear combination of local and global colonization (Eq. (2.1.1)). However, proportion of occupied patches monotonically increases as the proportion  $p$  of global colonization is increased (Figures 3.8, 3.9 and 3.10). In our model, total strength of local and global colonization has been normalized to be the same,  $c_{l0} = c_g$  in the unit space  $\Omega$ . In reality, however, this assumption is quite unlike to hold;  $c_{l0} > c_g$ . Exploring a wider parameter region for  $c_{l0} \neq c_g$  may result in the same results obtained in lattice space.

Point pattern approach is very flexible to represent *any* spatial distribution of local patches. Hence, there could be some further studies applying point pattern method to both theoretical problems and biological systems. In our model, all patches are identical in size and thus they have the same local extinction rate. In reality, however, we observe spatial metapopulations

where local patches with various areas/sizes are involved. This heterogeneity in patch size can be easily handled with our point pattern approach as follows: We assume a patch with a minimum size and represent it as a point, then a patch with a larger size is represented by a certain number of points that are spatially clustered within the range of local colonization so that it behaves as one large sized patch. The pair correlation function of such a point pattern  $g(r)$  would have a complicated functional form. But we can use it to analytically derive the equilibrium 1st and 2nd order structure of empty and occupied patches as we have shown for the three types of baseline point pattern (CSR, clumped and over-dispersed). Exploring our model on baseline point patterns for, e.g., islands-mainland metapopulation or metapopulation with a gradient in patch size, etc., is worth challenging. Since the equilibrium theory of island biogeography shares the same fundamental processes of colonization and extinction with the metapopulation idea, our approach of point pattern could be extended to revisit the equilibrium theory of island biogeography.

In our model, the status of a point is either empty or occupied. As a further extension of the present model, it is possible to introduce the 3rd status such as “permanently destroyed” or “temporarily barren”. The former corresponds to anthropogenic patch destruction and the latter corresponds to over-exploitation of natural resources by the occupant species. A permanently destroyed patch may be restored to empty so that the patch can be colonized again. A barren patch will become empty and can be occupied when natural resources recover after a certain time. Or we may introduce the 2nd species that always wins against species 1 so that both species never coexist within a patch. This situation can be modeled by extending the classical epidemic SIR (Susceptible - Infectious - Recovered) or SIRS (Susceptible - Infectious - Recoved - Susceptible) model to spatial point pattern dynamics. Further study with three status assigned to each point is worth exploring.

Regarding to the positions of points in point patterns, in the present model, points are assumed to be static in the sense that their locations are fixed. Another extension of metapopulation models which could be explored is that we allow points to be able to move, that means the point pattern is not static in those models. For instance, if we focus on the metapopulation of an ectoparasite which inhabits on animals’ fur or skin. As animals move, local patches also moves. In addition, animals can give birth and die then we also can consider the birth and death of points in the point pattern. Exploring the more complicated models where the positions of points are not fixed and the number of points does not remain constant with a certain rule is worth challenging.

On the other hand, in our model, one occupied patch goes to extinct with a constant rate  $e$ , that means the lifetime of an occupied patch is exponentially distributed. Specifically, we assume the local extinction rate  $e = 1$ , so  $1/e = 1$  and on average an occupied site remains occupied for unit time 1 but their distribution is exponential. This means that if there is no colonization and initially there is a certain number of occupied patches, then many of them are in quite short occupancy; in other words, after being occupied, they quickly become empty. In addition, the local extinction rate  $e$  corresponds to the recovery rate  $\gamma$  in epidemic dynamics such as classical SIS model, SEIS (Susceptible - Exposed - Infectious - Susceptible) or SIRS models. In those models, the average life of some infectious states is also exponential distributed, that means most of infected individuals quickly recover after infection, while some infected individuals remain being infectious for long period of time, but the average time is  $1/\gamma$ . However, in reality, especially for infectious diseases such as Covid 19 or Influenza, the recovery time is never exponential

distributed, ones usually have seen unimodal distribution. It is more realistic when after getting infected, a lot of people likely recover after a certain time. In the perspective of metapopulation dynamics, ignoring unimodality and assuming local extinction rate to be constant may be too simple to apply to real systems. Lately there are some researches on how the unimodality affects the spread of infectious diseases. It is shown that exponential distribution and unimodal distribution can have slightly different impacts on spread of infectious diseases. Then we might think about the case that the lifetime of an occupied patch shows a unimodal distribution in further studies of metapopulation models.

In a broader perspective, we also can apply point pattern method to many biological problems. Because plants do not move then we can apply point pattern dynamics to study the metapopulation models in plant ecology. In respect of terrestrial plant studies, for instance, we can apply point pattern approach to the study the dynamics of mistletoe, a species of hemiparasitic plants which are attached to their host trees and extract water and nutrients from the host plants. We can consider each host tree as a local patch or a point and study the distribution of host trees which are occupied by mistletoe over a space.

Besides, there are some interesting topics in regard to marine ecosystems which can be studied theoretically by applying point pattern dynamics. One idea is about the metapopulation of a special worm that is called tube worm inhabiting the skeletal remains of a dead whales on the sea floor. After a whale dies, its carcass falls to the seabed and if a whale carcass is found by an egg of this worm, it will be occupied. When the whale skeleton has been devoured the worms die. And after some time, the huge bones from whales disappear. The locations of whale's carcasses could be considered as a static point pattern then we can study how occupied dead whale bodies are distributed over space. In addition, we can study a little more complicated case in which the number of points can change with time when a whale carcass is completely dissolved or new dead whale body comes to the seabed.

Also relating to studies on biological systems of species living on the ocean floor, we can study the dynamics of hydrothermal vents, fissure on the seabed from which geothermally heated water discharges using point pattern dynamics. It is easy to find these vents commonly near such as volcanically active places or areas where tectonic plates are moving apart. There is a very special ecosystem and biological communities such as some species of tube worms or other organisms living around hydrothermal vents. These days, we have more and more precious data about where hydrothermal vents located. A set of vents can be described as a point pattern. The location of a vent is considered a local habitat under the deep sea and there might be dispersal or local extinction of species happening. In this case, the number of vents is fixed and the vents' locations do not change.

Theoretical studies of the metapopulation dynamics of those worms from the two examples above as point pattern dynamics are promising as it is impossible to do empirical studies of those worms under the deep sea and do observations for a long period of time. However, generally for a lot of studies, we can compare the results of theoretical problems on spatial metapopulation dynamics as point pattern dynamics with those of empirical studies and spatial point pattern analysis of real data.

# Conclusion

These days, anthropogenic activities have made an environment increasingly fragmented in which biological species inhabit; a habitat that was formerly continuously distributed over space is now fragmented into pieces of local habitats spatially separated to a lesser or a greater extent. Such a habitat of a spatial metapopulation is best described by a point pattern as a collection of local patches that are connected with each other by local and global colonization. With increasing awareness of the vulnerability of biodiversity in a fragmented habitat, spatial metapopulation dynamics needs to be studied so that relevant methods of management may be attempted to prevent complete extinction.

With the results we have gained from this research and other previous studies, we can say that the point pattern method is a useful and powerful tool to study spatial metapopulation models in ecology as well as biological problems in general. We appeal the versatility and usefulness of the point pattern approach to theoretically explored spatial population dynamics in the study of metapopulation, landscape and conservation ecology.

# Acknowledgement

First and foremost, I would like to express my deepest and sincere gratitude and appreciation to my supervisor, Prof. Fugo Takasu, who has given me a lot of constructive suggestions and advice, immense knowledge and warm encouragement. He is always patient, helpful and supportive during my entire process of doctoral course not only in academic aspects but also in life. This thesis is a result of his continuous guidance and supervision received by me for which I am extremely grateful.

I would also like to express my sincere thanks to Prof. Satoshi Takahashi of Department of Environmental Science for his helpful guidance and advice during the course of this study.

I also want to express my sincere gratitude to all the professors and members of Graduate School of Humanities and Sciences at Nara Women's University for their great support.

I would like to sincerely thank all members of International Division for their wonderful support to make my life go smoothly from my first day in Nara.

A very special thank to Dr. Trong-Hieu Nguyen of Hanoi University of Science in Vietnam for significant encouragement, helpful advice and suggestions before and during my doctoral course.

I would like to deeply thank the Ministry of Education, Culture, Sports, Science, and Technology (MEXT) for scholarship support so that I have had a great opportunity to study in Japan and pursue higher education.

A word of thanks also goes to my friends, laboratory members for kind support and useful advice.

Last but not least, I would also like to thank my parents and family for the support they have provided me throughout my entire life.

# Bibliography

- [1] Bolker, D. H., 1999. Analytic Models for the Patchy Spread of Plant Disease. *Bulletin of Mathematical Biology* 61, 849-874.
- [2] Brown, D. H., Bolker, B. M., 2004. The Effects of Disease Dispersal and Host Clustering on the Epidemic Threshold in Plants. *Bulletin of Mathematical Biology* 66, 341-371.
- [3] Brown, J. H., Kodric-Brown, A., 1977. Turnover rates in insular biogeography: Effect of immigration on extinction. *Ecology* 58, 445-449.
- [4] Cornell, S. J., Ovasakainen, O., 2008. Exact asymptotic analysis for metapopulation dynamics on correlated dynamic landscapes. *Theoretical Population Biology* 74 (3), 209-225.
- [5] Cornell, S. J., Suprunenko, Y. F., Finkelshtein, D. et al., 2019. A unified framework for analysis of individual-based models in ecology and beyond. *Nature Communications* 10, 4716.
- [6] Dale, M. R. T., John, E. A., 1999. Neighbour diversity in lichen-dominated communities. *Journal of Vegetation Science* 10 (4), 571-578.
- [7] Dieckmann, U., Law, R., 2000. Relaxation projections and the method of moments. In: Dieckmann, U., Law, R., Metz, J.A.J. (Eds.), *The Geometry of Ecological Interactions: Simplifying Spatial Complexity*. Cambridge University Press, 412-455.
- [8] Diggle, P. J., 2003. *Statistical Analysis of Spatial Point Patterns*. Hodder Education.
- [9] Gillespie, D. T., 1976. A General Method for Numerically Simulating the Stochastic Time Evolution of Coupled Chemical Reactions. *Journal of Computational Physics* 22, 403-434.
- [10] Hamada, M., Takasu, F., 2019. Equilibrium properties of the spatial SIS model as a point pattern dynamics - How is infection distributed over space?. *Journal of Theoretical Biology* 468, 12-26.
- [11] Hanski, I. A., 1983. Coexistence of competitors in patchy environment. *Ecology*, 64, 493-500.
- [12] Hanski, I. A., 1985. Single-species spatial dynamics may contribute to long-term rarity and commonness. *Ecology* 66, 335-343.

- [13] Hanski, I. A., 1991. Single-species metapopulation dynamics: concepts, models and observations. *Biological Journal of the Linnean Society* 42 (1-2), 17-38.
- [14] Hanski, I. A., 1998., Metapopulation dynamics. *Nature* 396, 41-49.
- [15] Hanski, I. A., 2011. Eco-evolutionary spatial dynamics in the Glanville fritillary butterfly. *PNAS* 108 (35), 14397-14404.
- [16] Hanski, I. A., Gilpin, M., 1991. Metapopulation dynamics: brief history and conceptual domain. *Biological Journal of the Linnean Society* 42 (1-2), 3-16.
- [17] Hanski, I. A., Gyllenberg, M., 1993. Two general metapopulation models and the core-satellite species hypothesis. *The American Naturalist* 142, 17-41.
- [18] Harada, Y., 1999. Short- vs. Long-range Disperser: the Evolutionarily Stable Allocation in a Lattice-Structured Habitat. *Journal of Theoretical Biology*, 201 (3), 171-187.
- [19] Harada, Y, Iwasa, Y., 1994. Lattice population dynamics for plants with dispersing seeds and Vegetative propagation. *Researches on Population Ecology* 36, 237-249.
- [20] Harrison, S. P., Taylor, A. D., 1997. Empirical evidence for metapopulation dynamics. In: Hanski, I., Gilpin, M. (Eds.), *Metapopulation Biology*. Academic Press, 27-42.
- [21] Hastings, A., 1991. Structured models of metapopulation dynamics. *Biological Journal of the Linnean Society* 42, 57-71.
- [22] Iwasa, Y., 2000. Lattice models and pair approximation in ecology. In: Dieckmann, U., Law, R., Metz, J.A.J. (Eds.), *The Geometry of Ecological Interactions: Simplifying Spatial Complexity*. Cambridge University Press, 227-251.
- [23] Kaito, C., Dieckmann, U., Sasaki, A., Takasu, F., 2015. Beyond pairs: Definition and interpretation of third-order structure in spatial point patterns. *Journal of Theoretical Biology*. 372, 22-38.
- [24] Levin, S.A., 1992. The Problem of Pattern and Scale in Ecology: The Robert H. MacArthur Award Lecture. *Ecology* 73 (6), 1943-1967.
- [25] Levins, R., 1969. Some Demographic and Genetic Consequences of Environmental Heterogeneity for Biological Control. *Bulletin of the Entomological Society of America* 15, 237-240.
- [26] Liebhold, A.M., Gurevitch, J., 2002. Integrating the Statistical Analysis of Spatial Data in Ecology. *Ecography* 25 (5), 553-557.
- [27] Matsuda, H., Ogita A., Sasaki A., Sato, K., 1992. Statistical mechanics of population: The lattice Lotka-Volterra model. *Progress in Theoretical Physics* 88 (6), 1035-1049.

- [28] North, A. R., Godfray, H. C. J, 2017. The dynamics of disease in a metapopulation: The role of dispersal range. *Journal of Theoretical Biology*, 418, 57-65.
- [29] Ovaskainen, O., Cornell, S. J., 2006a. Asymptotically exact analysis of stochastic metapopulation dynamics with explicit spatial structure. *Theoretical Population Biology* 69 (1), 13-33.
- [30] Ovaskainen, O., Cornell, S. J., 2006b. Space and stochasticity in population dynamics, *PNAS* 103 (34), 12781-12786.
- [31] Ovaskainen, O., Finkelshtein, D., Kutoviy, O., Cornell S., Bolker, B., Kondratiev, Y., 2014. A general mathematical framework for the analysis of spatiotemporal point processes. *Theoretical Ecology* 7, 101-113.
- [32] Sato K., Iwasa, Y., 2000. Pair Approximations for Lattice-based Ecological Models. In: Dieckmann, U., Law, R., Metz, J.A.J. (Eds.), *The Geometry of Ecological Interactions: Simplifying Spatial Complexity*. Cambridge University Press, 341-358.
- [33] Sato, K., Matsuda, H., Sasaki, A., 1994. Pathogen invasion and host extinction in lattice structured populations. *Journal of Mathematical Biology* 32, 251-268.
- [34] Turner, M.G., 1989. Landscape Ecology: The Effect of Pattern on Process. *Annual Review of Ecology and Systematics*. 20 (1), 171-197.
- [35] van Nouhuys, S., 2016. *Metapopulation ecology*, eLS. John Wiley & Sons, Ltd.
- [36] Wright, S., 1946. Isolation by distance under diverse systems of mating. *Genetics* 31 (1), 39.